The chemistry of astrophysical environments:

Synergies between far-infrared spectroscopy & laboratory experiments and future directions

814. Wilhelm and Else Heraeus Seminar:

Heritage of SOFIA – Scientific Highlights and Future Perspectives

2024 April 24

Helmut Wiesemeyer

MAX PLANCK INSTITUTE FOR RADIO ASTRONOMY

with Rolf Güsten, Paul Hartogh, H.W. Hübers & David A. Neufeld

*GREAT*ful acknowledgments: SOFIA Science & Operations Centers, DSI, GREAT Team

Outline

- Helium hydride (HeH^+), the first heteromolecular bond of the universe, and potentially important coolant.

- Jupiter's deuterium fraction, a relic from the protosolar nebula.

- The $^{16}O/^{18}O$ ratio in Earth's upper atmosphere and isotopic exchange reactions.

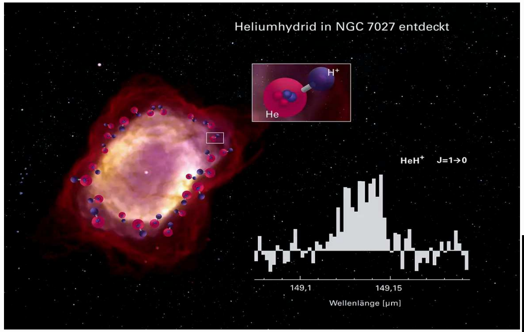

© NIESYTO design/ Latter/ CalTech/ NASA/ Güsten

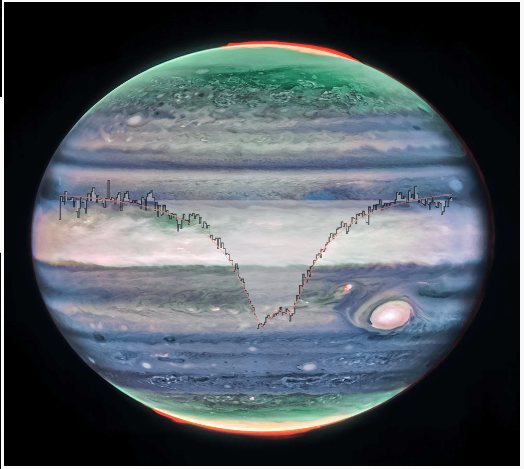

© NASA/ STScI, Wiesemeyer et al. (2024)

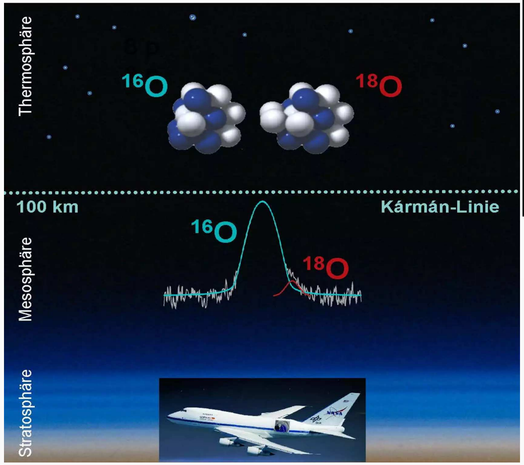

© Wiesemeyer et al./ NASA/ DSI (Stéphane Guisard & NIESYTO design)/ Simmon (NASA GSFC)

Cosmic evolution

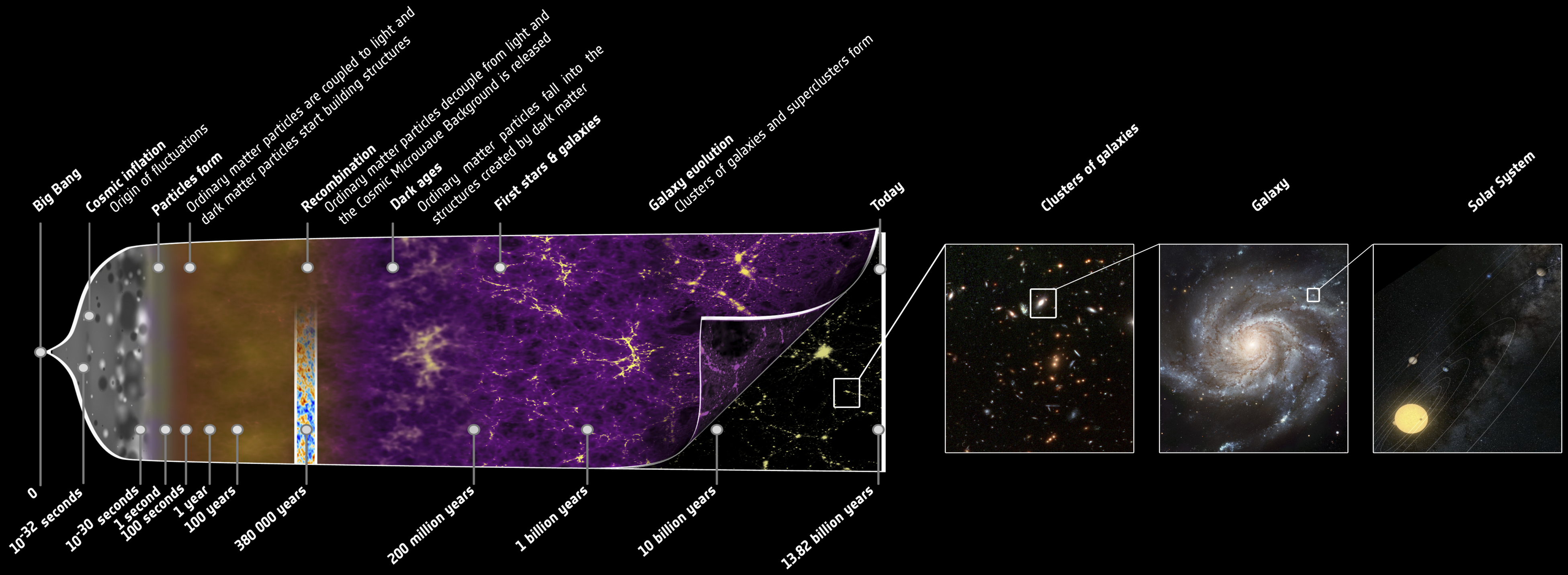

z = 1000 125 6 0.33

Cosmic evolution

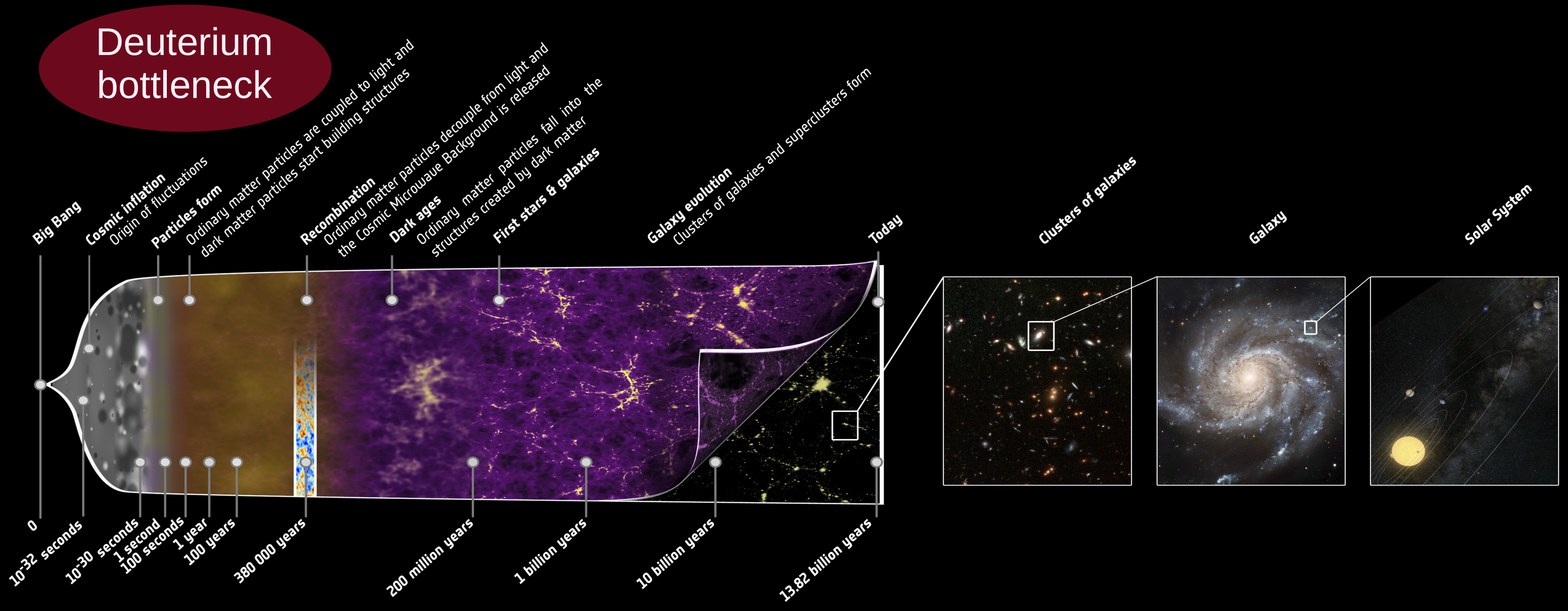

z = 1000 125 6 0.33

Cosmic evolution

Deuterium bottleneck

3α process vs. ^{8}Be decay

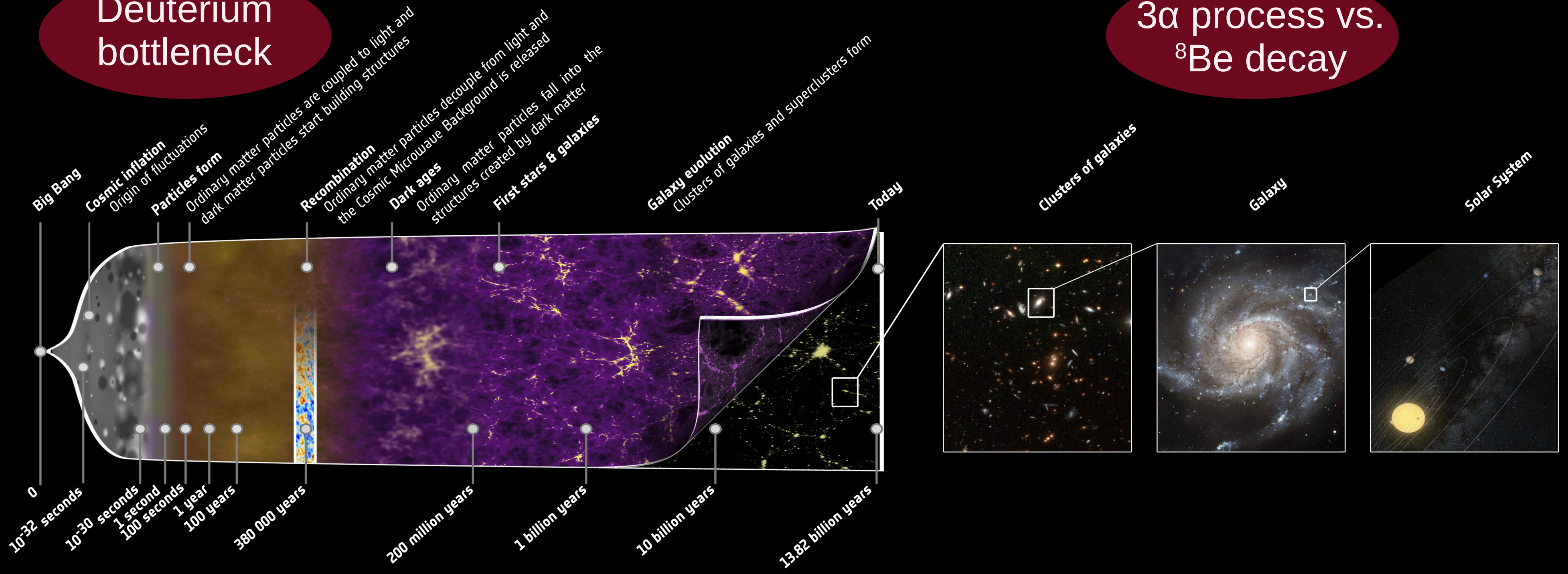

z = 1000 125 6 0.33

I. Helium hydride (HeH^+), first heteromolecular bond of the universe

(Güsten+ 2019, Nature 568; Neufeld+ 2020, ApJ 894)

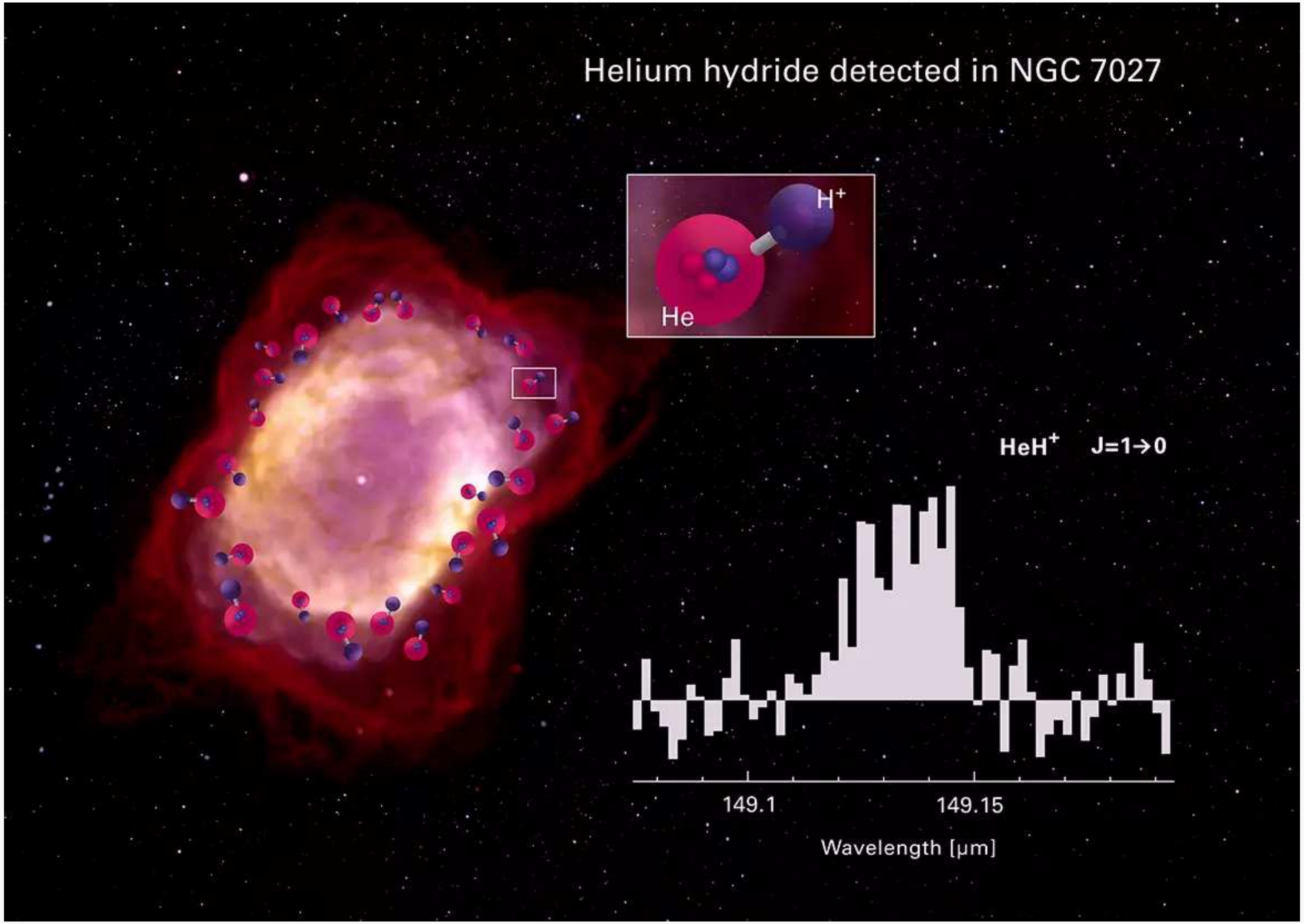

© NIESYTO design/ Latter/ CalTech/ NASA/ Güsten

Cloudy modeling of ionization and chemical structure

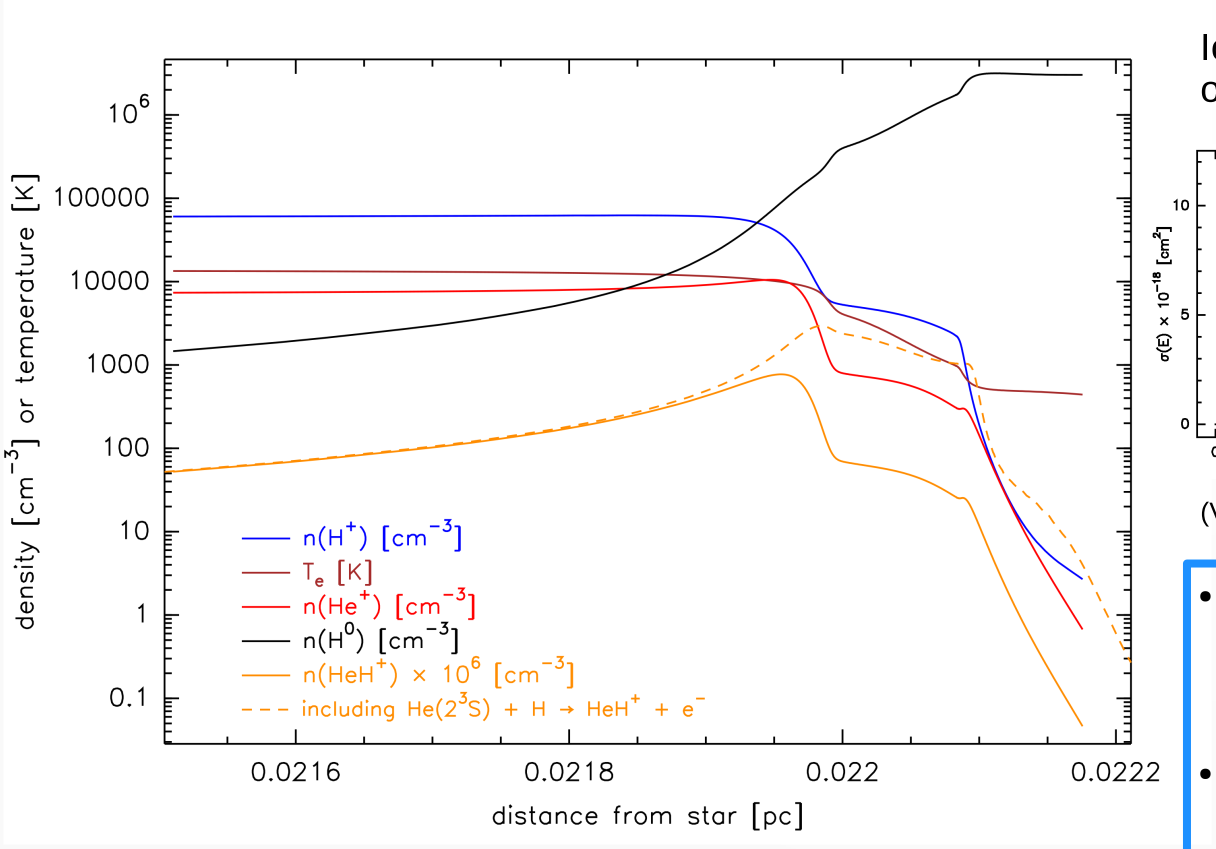

CLOUDY *C17.02*, Ferland et al. (2017)

Ionization cross-sections of H, He, He$^+$ and O:

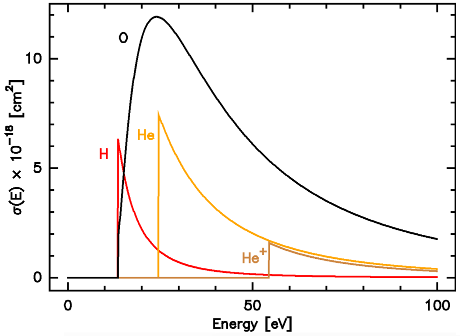

(Verner+ 1996, ApJ 465)

Ratio of modeled/ observed line fluxes:

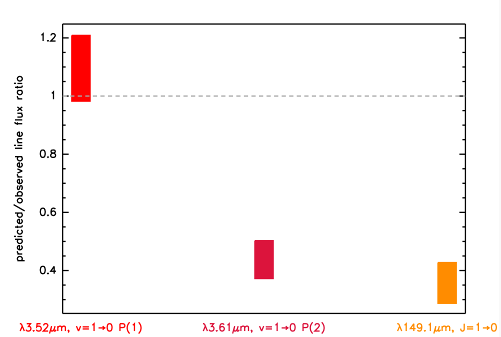

(from Neufeld+ 2020, ApJ 894)

- Cloudy modeling of constant-pressure HII region reproduces λ3.5 μm line flux [v=1-0 P(1)], but underestimates P(2) & J = 1-0 lines.
- Possible explanations:
  (1) Patchy structure of HII region.
  (2) Uncertainties in reaction rates.

Why ionization-bounded planetary nebulae matter

HeH^+ shell in NGC 7027 and cosmological matter/radiation decoupling in comparison:

	NGC7027	redshift 2600
T [K]	5100	7100
n_H [cm^{-3}]	2.6×10^5	7400
P/k [K cm^{-3}]	1.6×10^9	5.3×10^7
$\int_{\nu_{Ly}}^{\infty} I_\nu d\nu$ [ergs^{-1}cm^{-2}sr]	160	20
n_e [cm^{-3}]	5960	7080
$n(He^+)n(H^0)k_1$ [cm^{-3}s^{-1}]	2.9×10^{-8}	3.6×10^{-18}
$n(He^0)n(H^+)k_2$ [cm^{-3}s^{-1}]	2.0×10^{-12}	1.6×10^{-14}

- Main formation pathway in PNe is radiative association of He^+ and H^0 in overshooting HeII layer.
- Secondary pathway: associative ionization of metastable He (2^3S).
- Destruction pathways the same as in early universe.

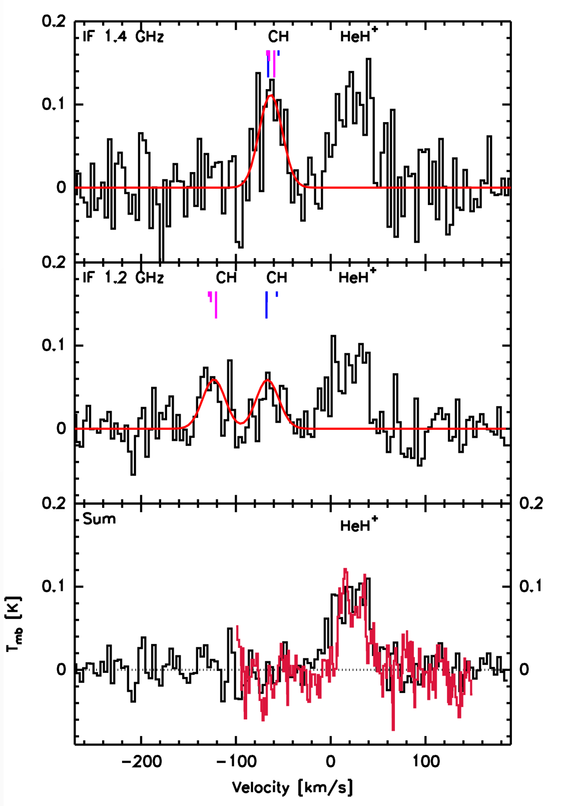

▲ HeH^+ (J=1-0, v=0 @ λ149 μm, P1 @ λ 3.52 μm)
Güsten et al. (2019), Neufeld et al. (2020)

Chemical evolution of the Universe from recombination to reionization (z=7.68*)

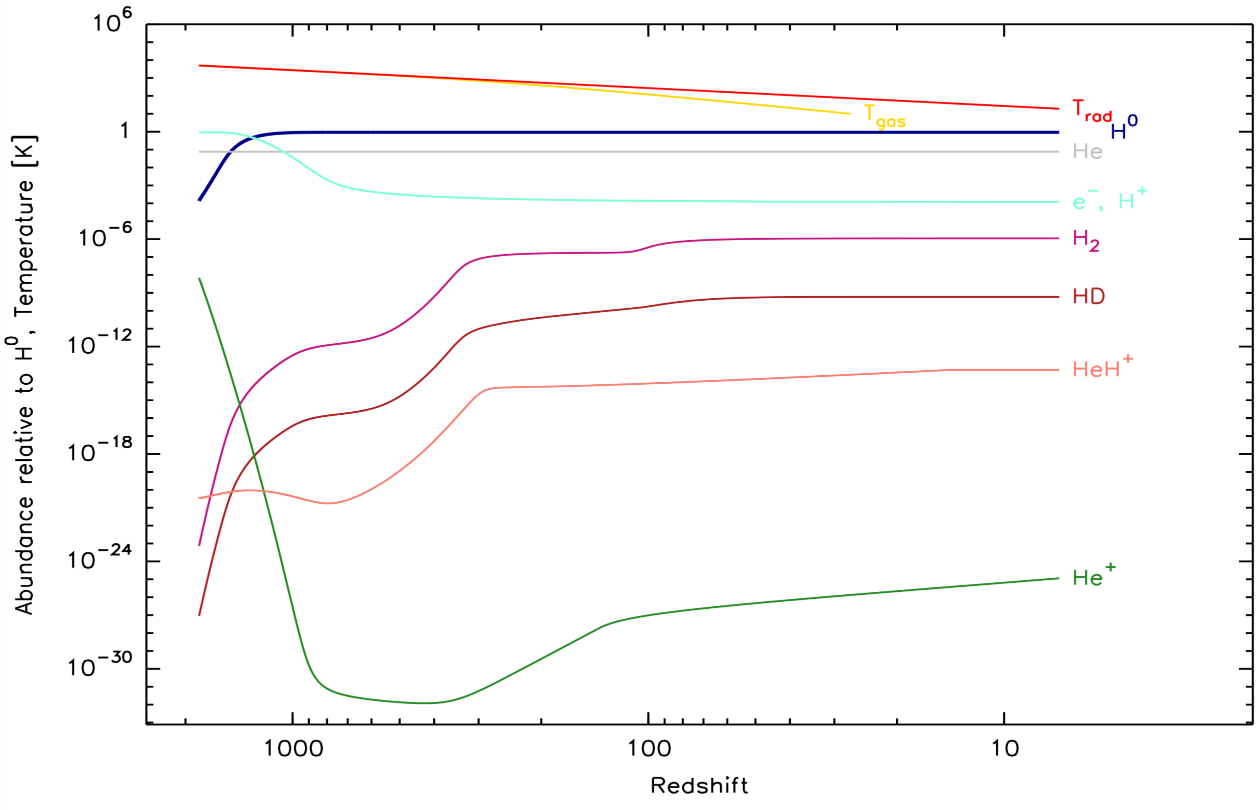

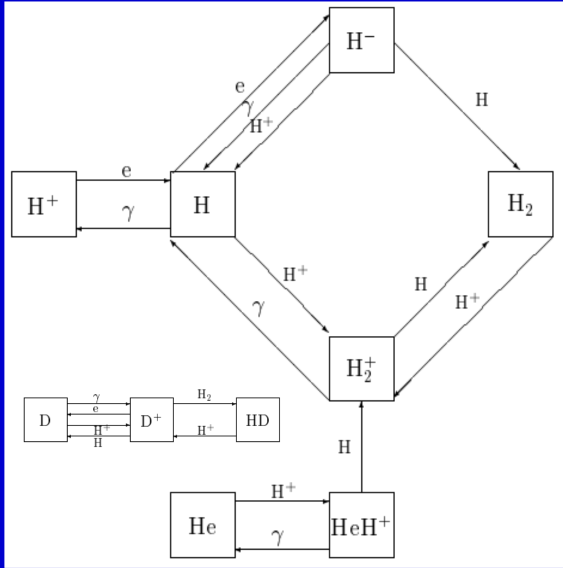

From Galli & Palla (1998, H_2 cooling).
Reprocessed* with recent reaction rates &

H_0	= 67.4 km s^{-1} Mpc^{-1}
Ω_b	= 0.049
Ω_{DM}	= 0.264
Ω_{vac}	= 1-Ω_M
$T_{cmb,0}$	= 2.7255 K
D/H	= 2.527 × 10^{-5}

*Planck 2018 results, *Cosmological parameters* (2020), KROME package v14.08

HeH⁺ as a prominent coolant?

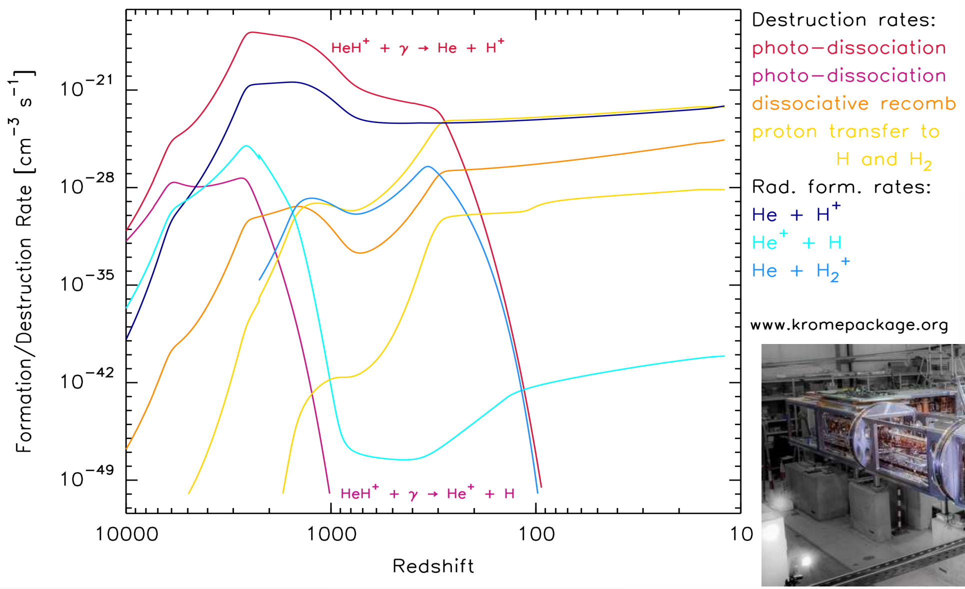

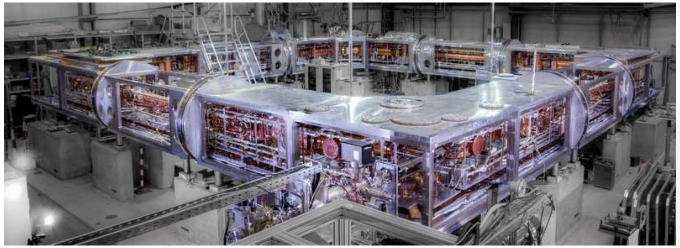

Cryogenic storage ring, MPI Nuclear Physics

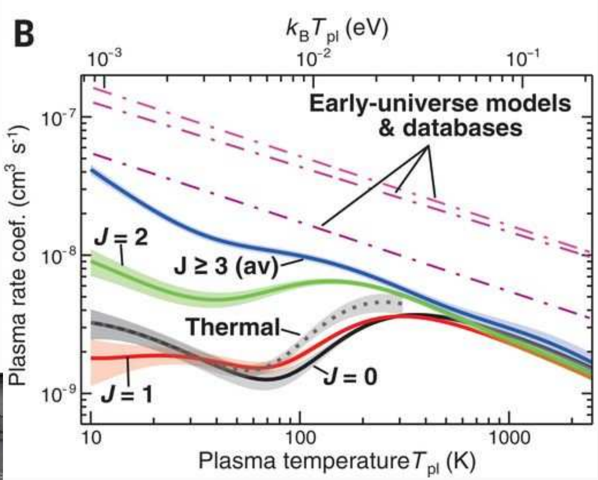

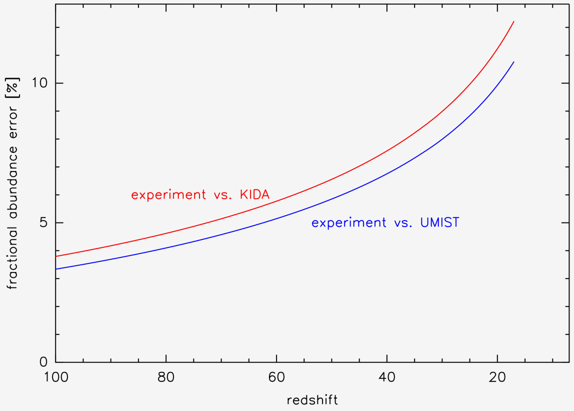

State-resolved dissociative recombination rate suggests primordial HeH^+ abundance larger than predicted by early-universe models (e.g., Galli & Palla 1998, 2013). [B]Novotný et al.,2019, Science 365

J-resolved rate for $He + H^+$: Factor ~100 at z=10 (Courtney+ 2021).

Thermal evolution of the Universe: from recombination to reionization

$$\frac{dT_m}{dt} = -2\,T_m H_0 (1+z)\sqrt{1+\Omega_0 z} + \frac{32\,\sigma_{sb} T_r^4}{3\,m_e c^2} x_e (T_r - T_m) + \frac{2(\Gamma_{mol} - \Lambda_{mol})}{3\,n\,k_b} + \frac{2\Theta_{ch}}{3\,n\,k_b} - \frac{T_m}{n}\left(\frac{dn}{dt}\right)_{ch}$$

(Peebles 1968, Puy et al. 1993)

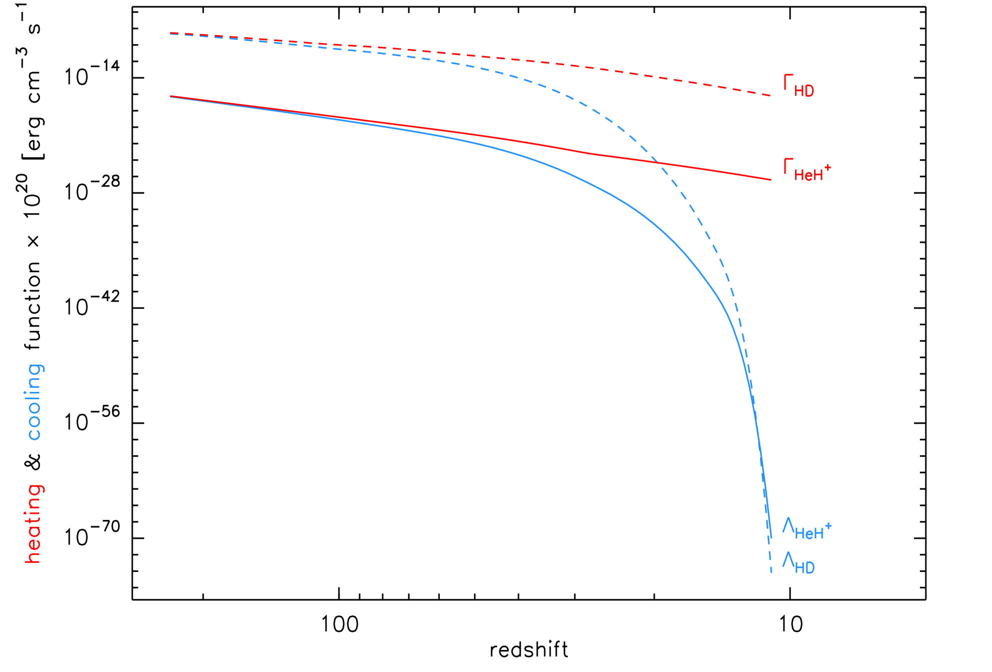

Heating and cooling functions for HD and HeH⁺

(inelastic collision rates: Desrousseaux, Lique et al. 2018,2020)

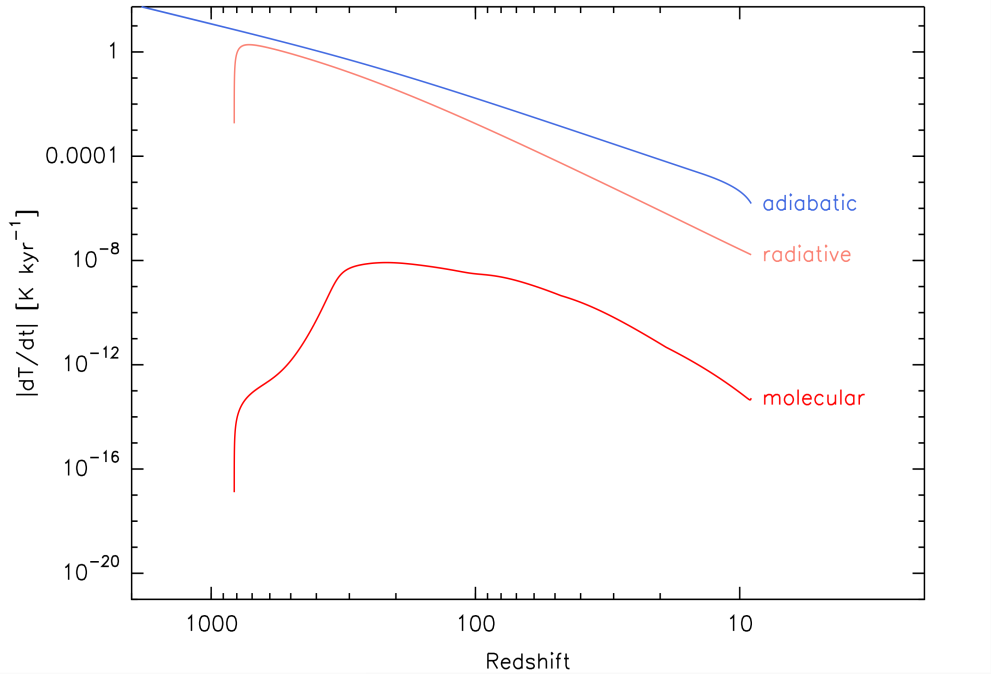

Heating and cooling of the young universe

(KROME package v. 14.0, Grassi et al. 2014)

Thermal evolution of the Universe: from recombination to reionization

$$\frac{dT_m}{dt} = -2T_m H_0(1+z)\sqrt{1+\Omega_0 z} + \frac{32\sigma_{sb}T_r^4}{3m_e c^2}x_e(T_r - T_m) + \frac{2(\Gamma_{mol}-\Lambda_{mol})}{3nk_b} + \frac{2\Theta_{ch}}{3nk_b} - \frac{T_m}{n}\left(\frac{dn}{dt}\right)_{ch}$$

(Peebles 1968, Puy et al. 1993)

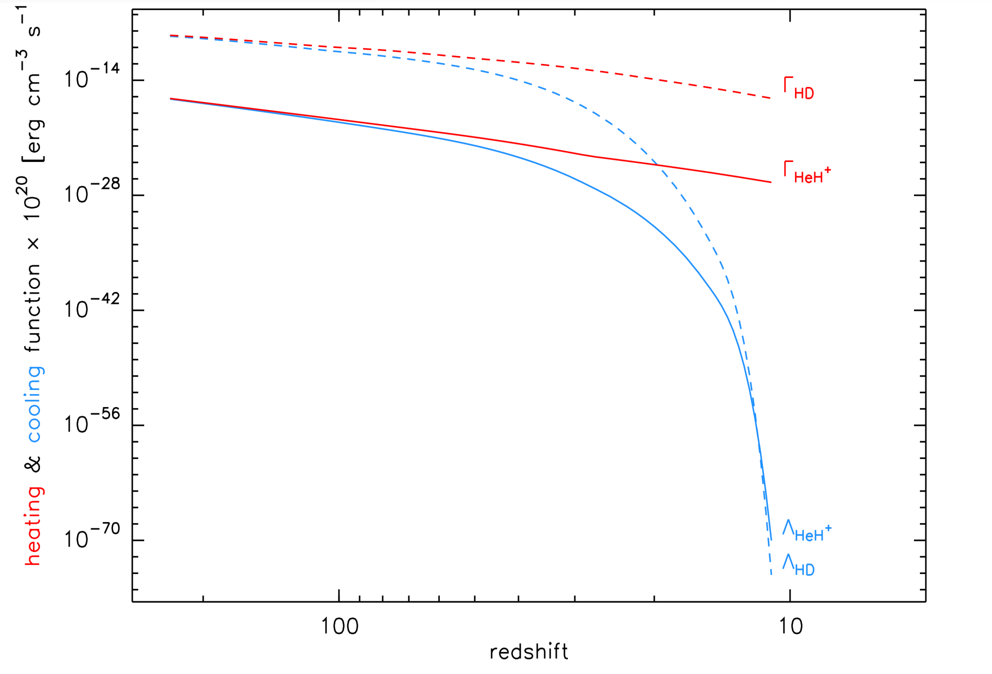

Heating and cooling functions for HD and HeH^+
(inelastic collision rates: Desrousseaux, Lique et al. 2018,2020)

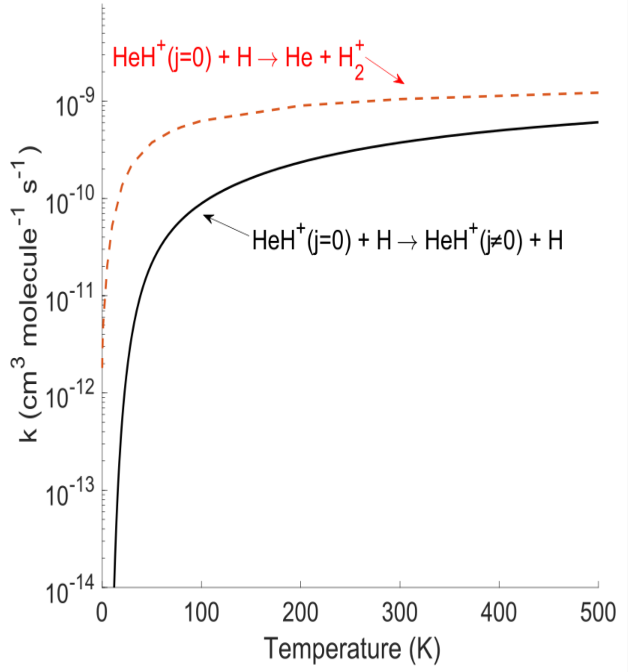

Inelastic and reactive collision rates* of ground-state HeH^+ (Desrousseaux & Lique 2020)

*final-state averages

HD and HeH^+ as coolants: Towards Population III Stars

(z ≈ 30 to z ≈ 5, Klessen & Glover 2023)

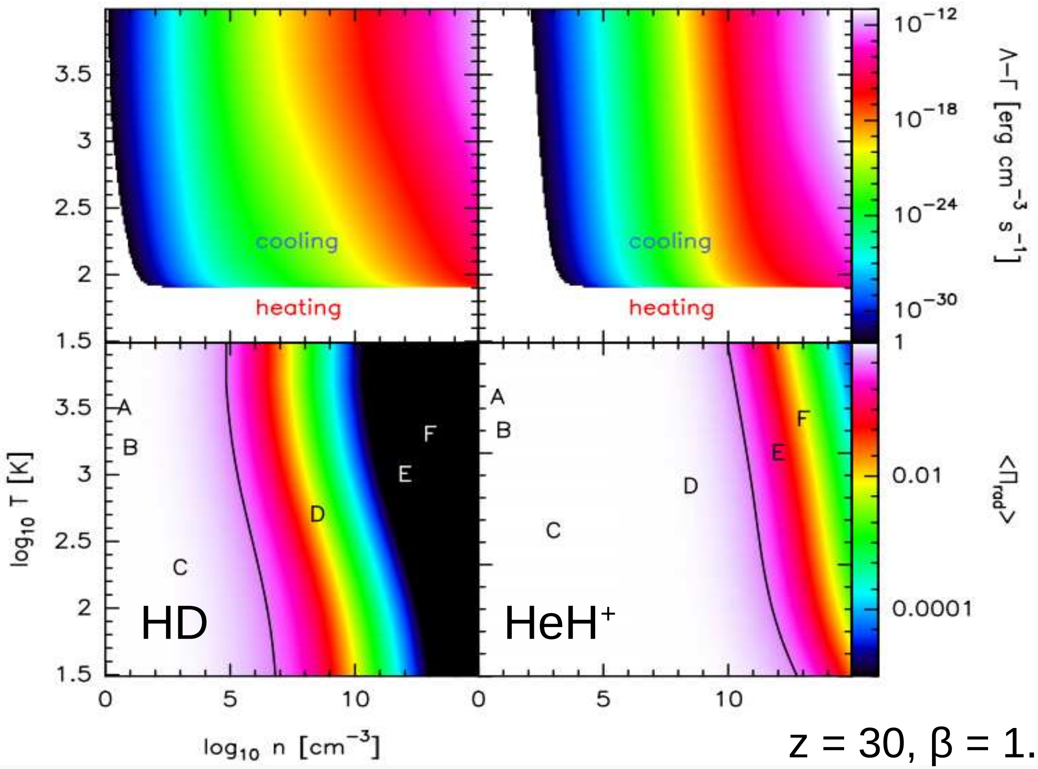

z = 30, β = 1.0

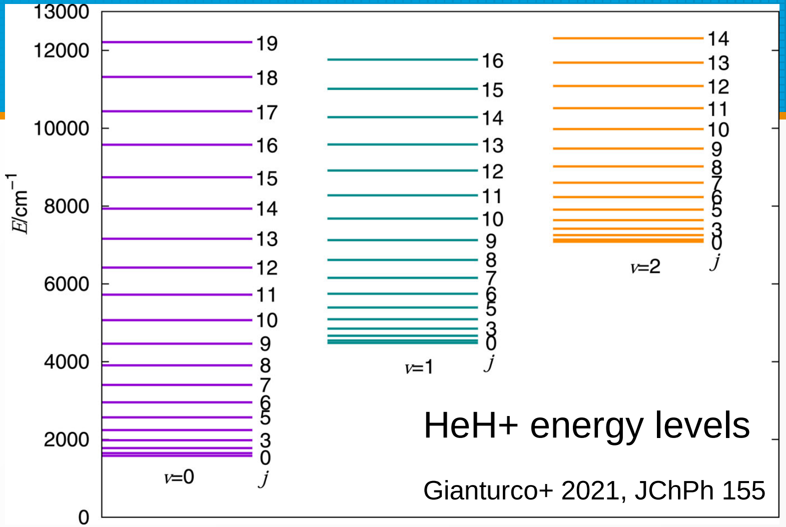

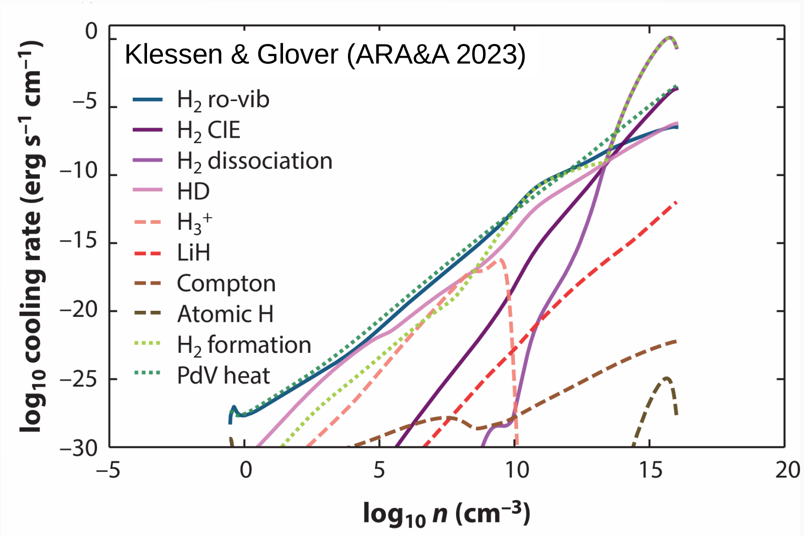

A: Compressionally heated flow into dark-matter halo.
B ► C: Runaway H_2 cooling.
C ► D: PdV heating.
E: Gas fully molecular.

HD and HeH^+ as coolants: Towards Population III Stars

(z ≈ 30 to z ≈ 5, Klessen & Glover 2023)

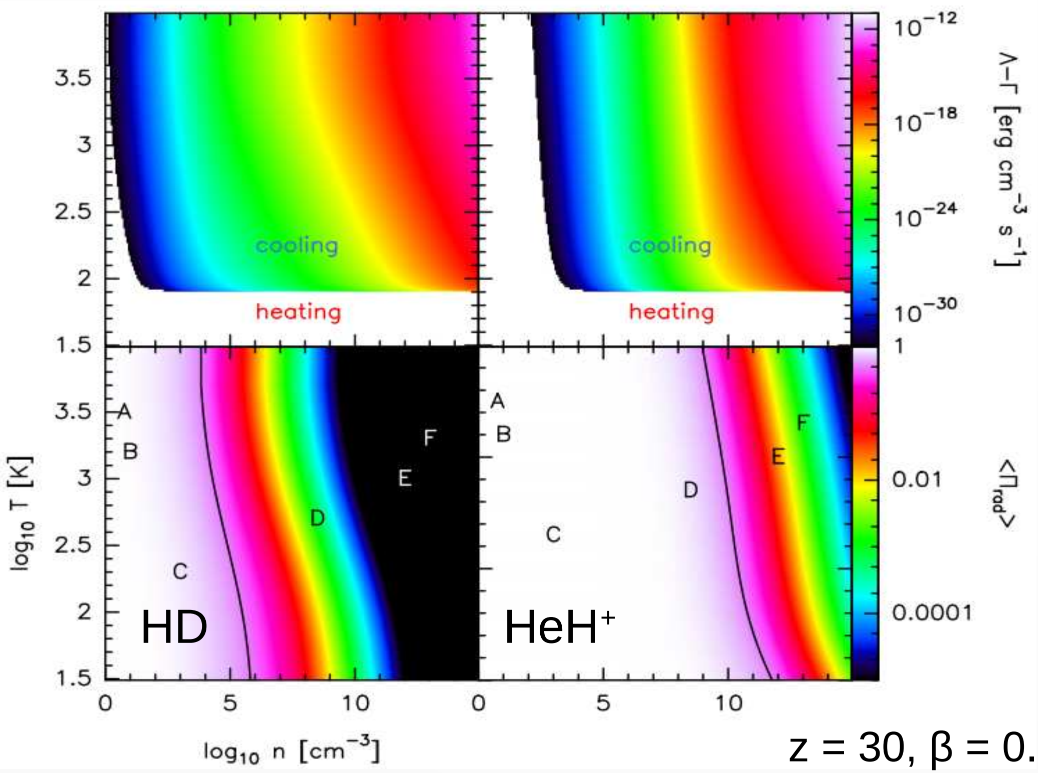

z = 30, β = 0.1

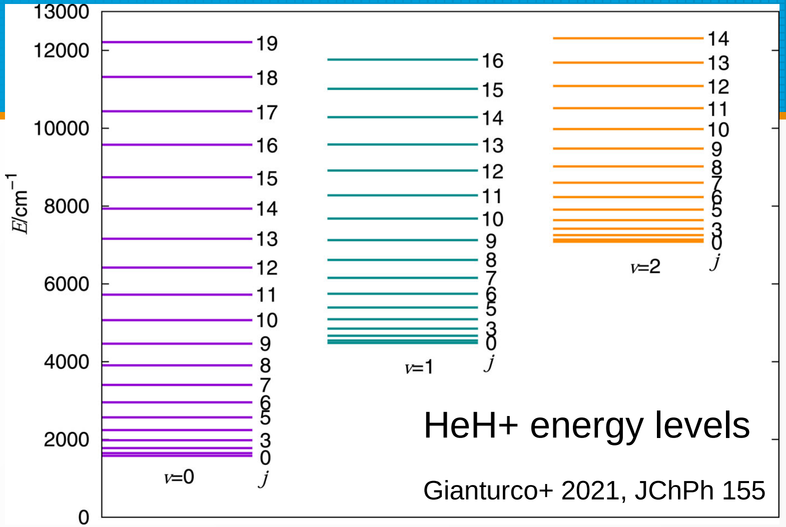

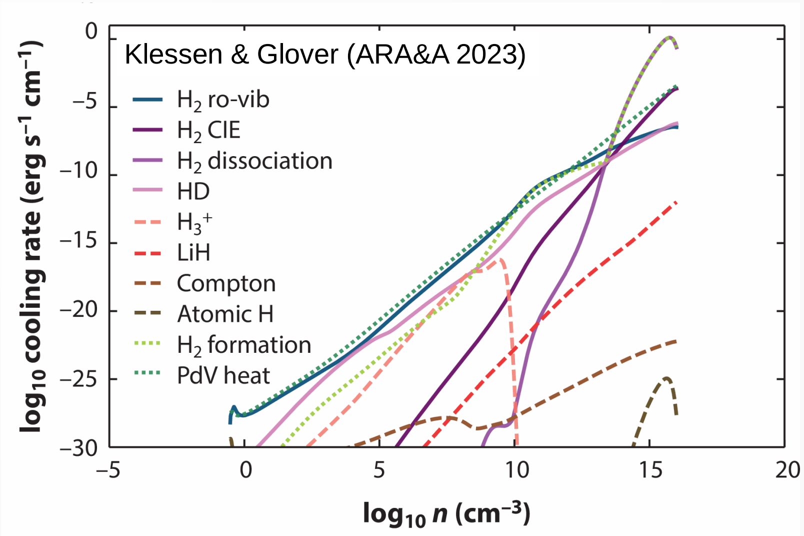

A: Compressionally heated flow into dark-matter halo.

B ► C: Runaway H_2 cooling.

C ► D: PdV heating.

E: Gas fully molecular.

HD and HeH^+ as coolants: Towards Population III Stars

(z ≈ 30 to z ≈ 5, Klessen & Glover 2023)

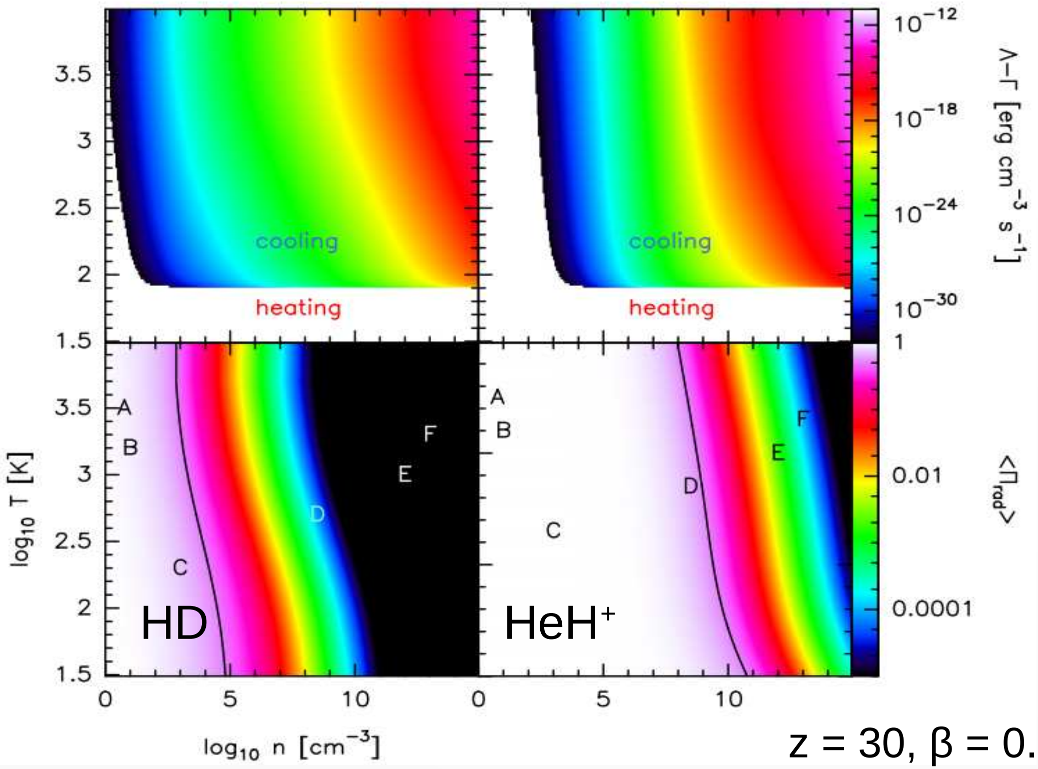

z = 30, β = 0.01

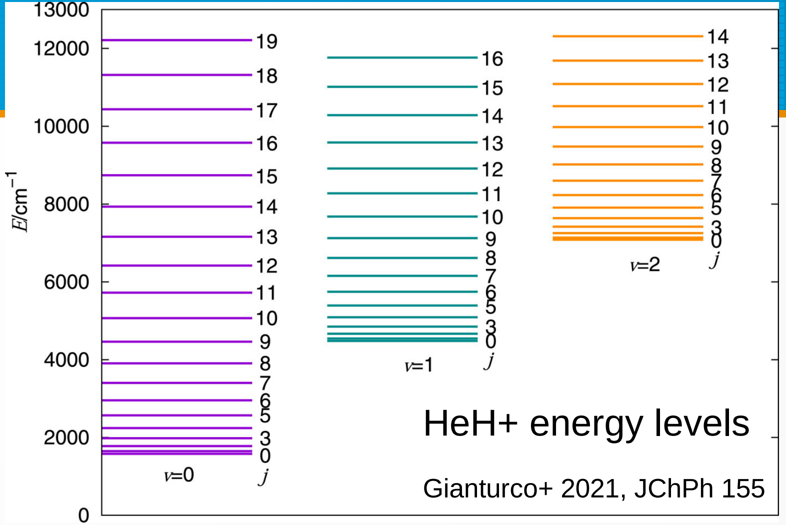

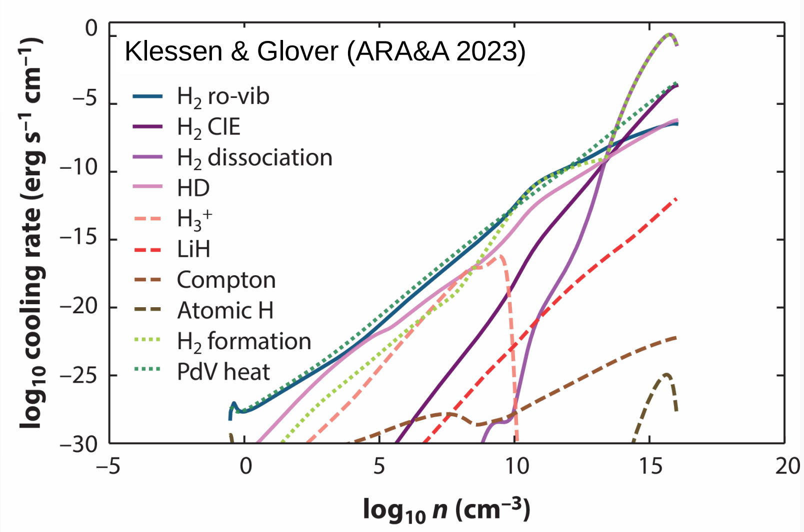

A: Compressionally heated flow into dark-matter halo.

B ► C: Runaway H_2 cooling.

C ► D: PdV heating.

E: Gas fully molecular.

II. Jupiter's deuterium fraction, a relic from the protosolar nebula

Wiesemeyer+ 2024, A&A in press

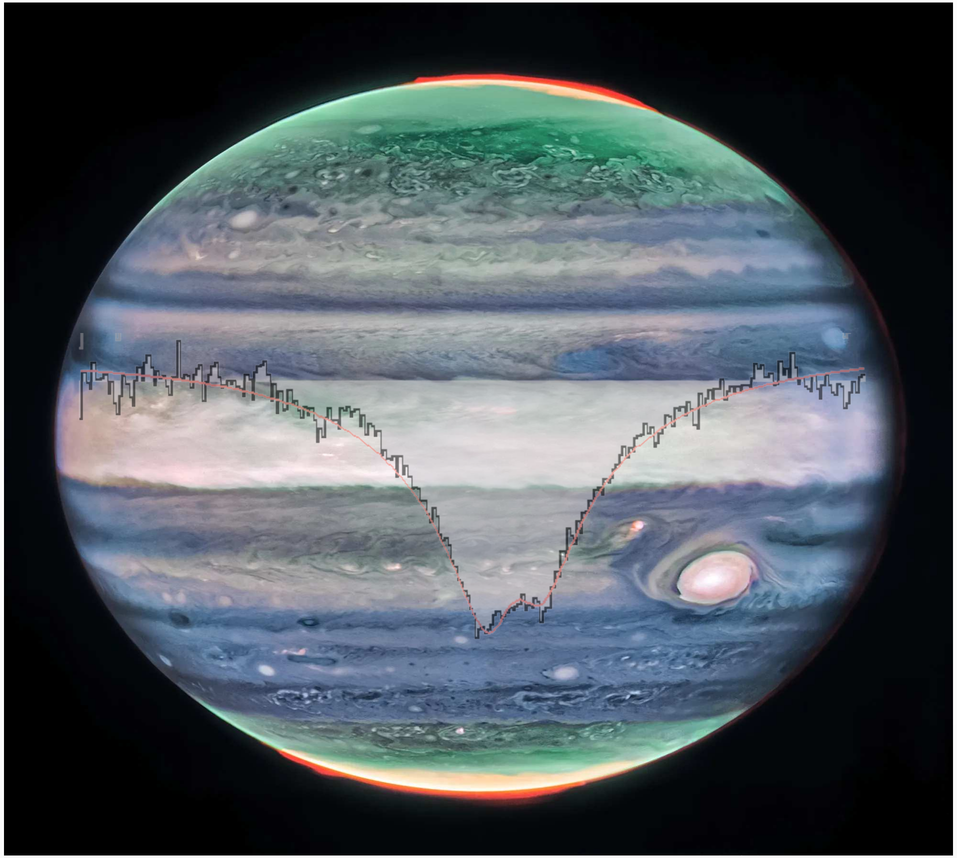

© NASA/ STScI, Wiesemeyer et al. (2024)

HD (J=1-0) as tracer of the Jovian deuterium fraction

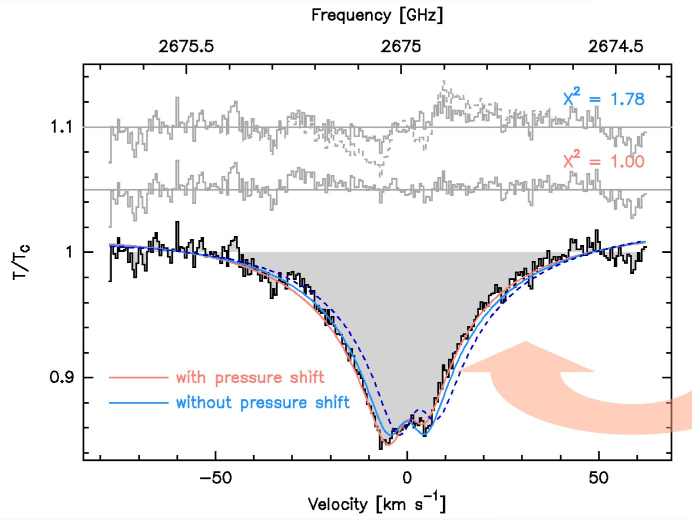

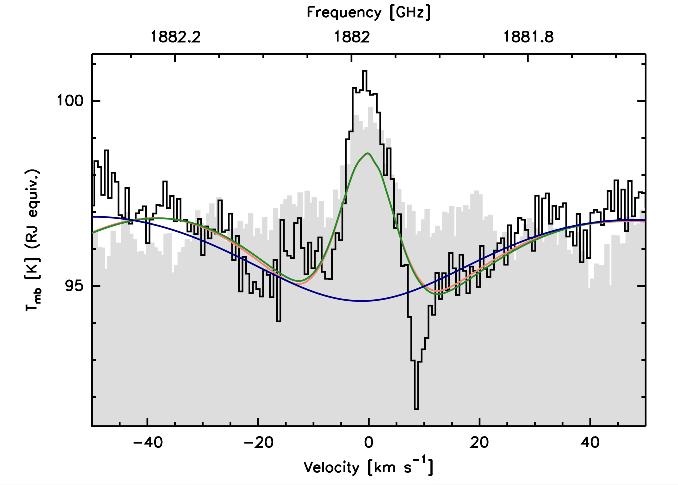

Left: HD, J=1-0 absorption (observed by 4G4, modeled without & with pressure shift).

Center: SOLEIL synchrotron, AILES beamline (collisional broadening of HD by H_2, Sung et al. 2023).

Right: CH_4 J=6-5 line with (green) & without (blue) stratospheric emission component (upGREAT & HIFI).

HD (J=1-0) as tracer of the Jovian deuterium fraction

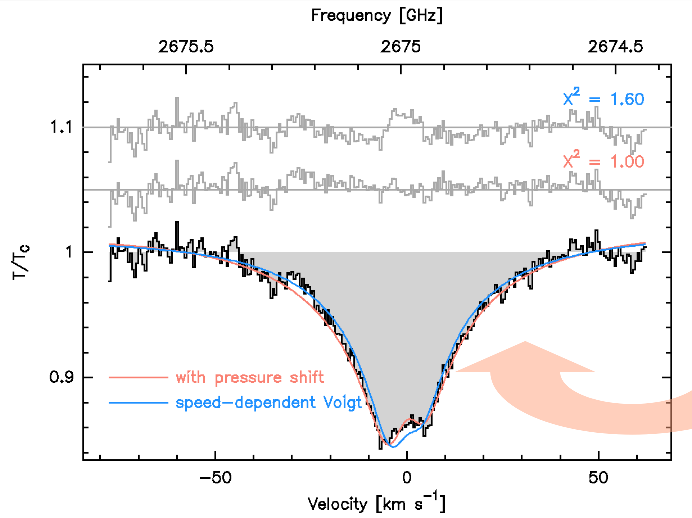

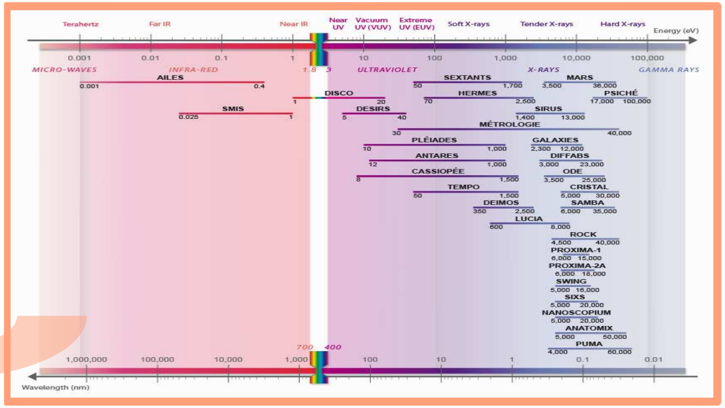

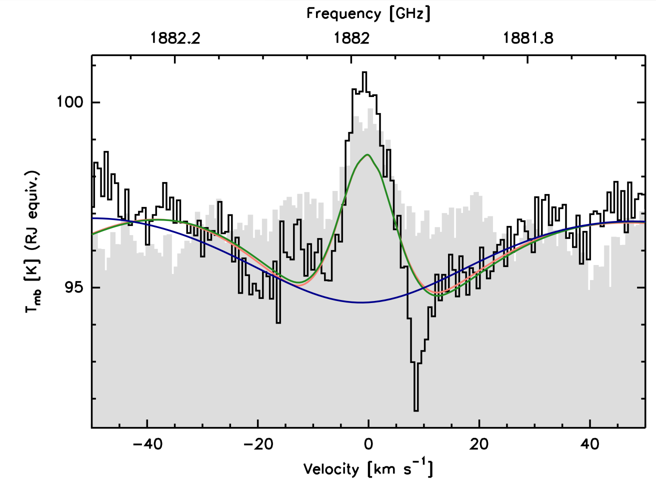

Left: HD, J=1-0 absorption (observed by 4G4, model with experimental & theoretical* pressure shifts).

Center: SOLEIL synchrotron, AILES beamline (collisional broadening of HD by H_2, Sung et al. 2023).

Right: CH_4 J=6-5 line with (green) & without (blue) stratospheric emission component (upGREAT & HIFI).

* Stankiewicz et al. 2021, HD/He system

Vertical abundance and transmission profiles of Jupiter's atmosphere

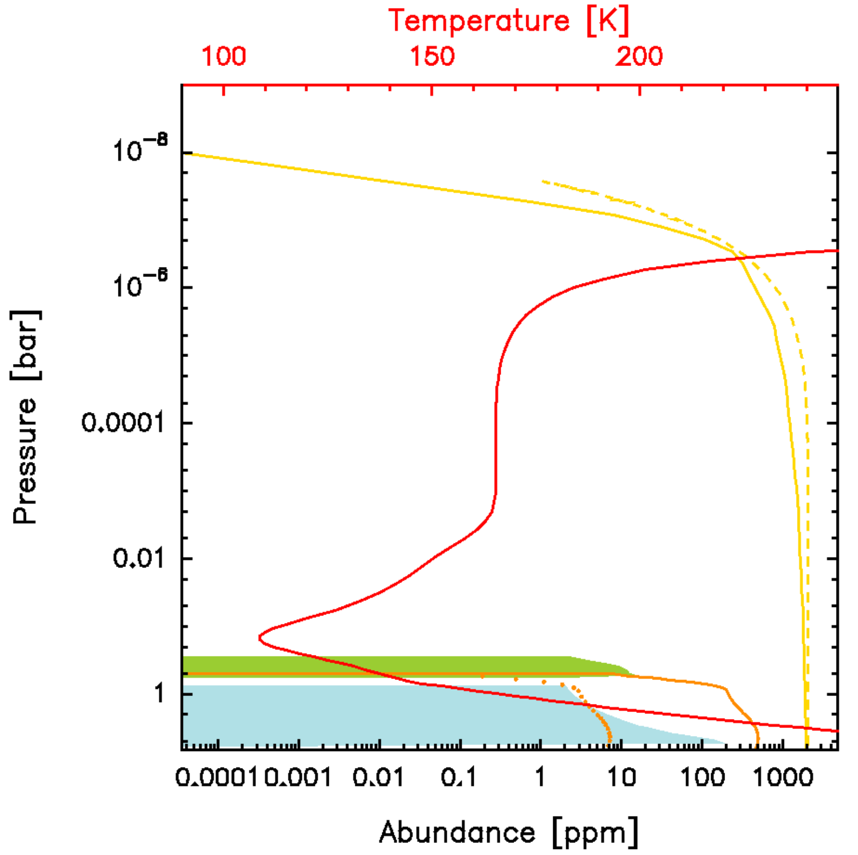

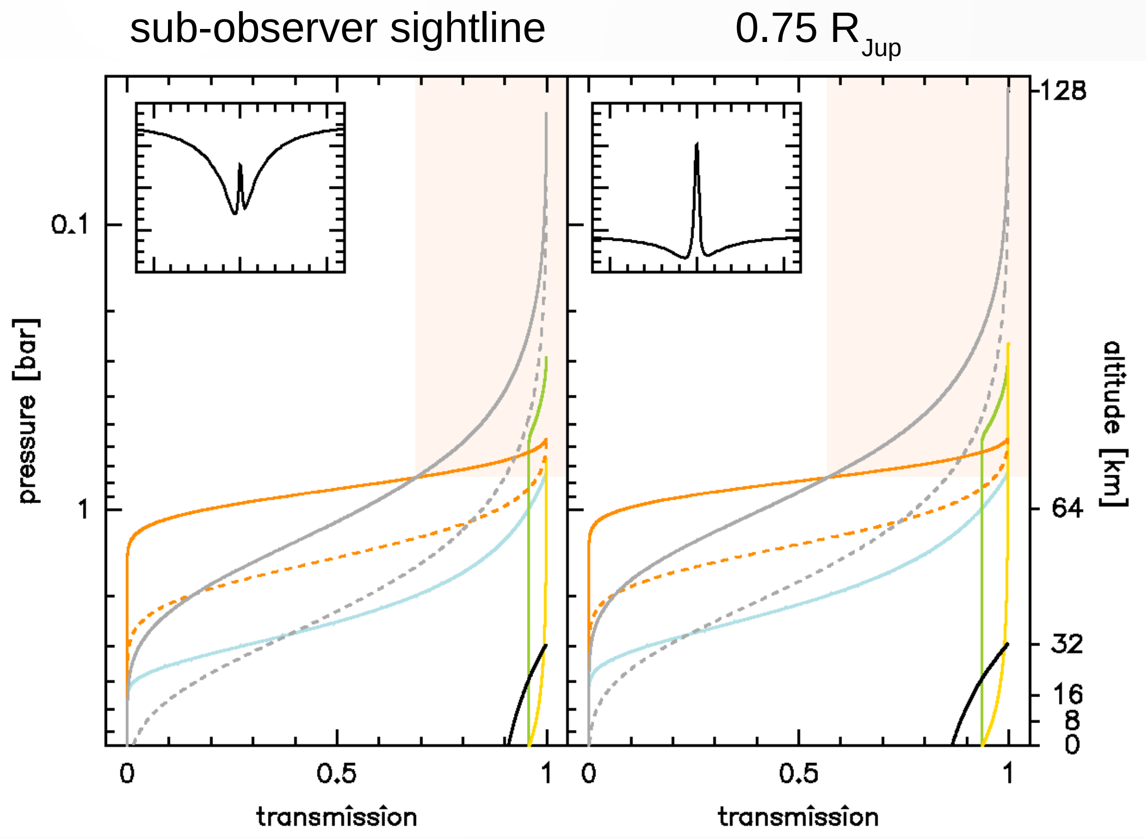

CH_4, NH_3 —, PH_3 ---, ammonia ice, water ice

Wiesemeyer et al. 2024, A&A in press

Synopsis of cosmic deuterium fractions

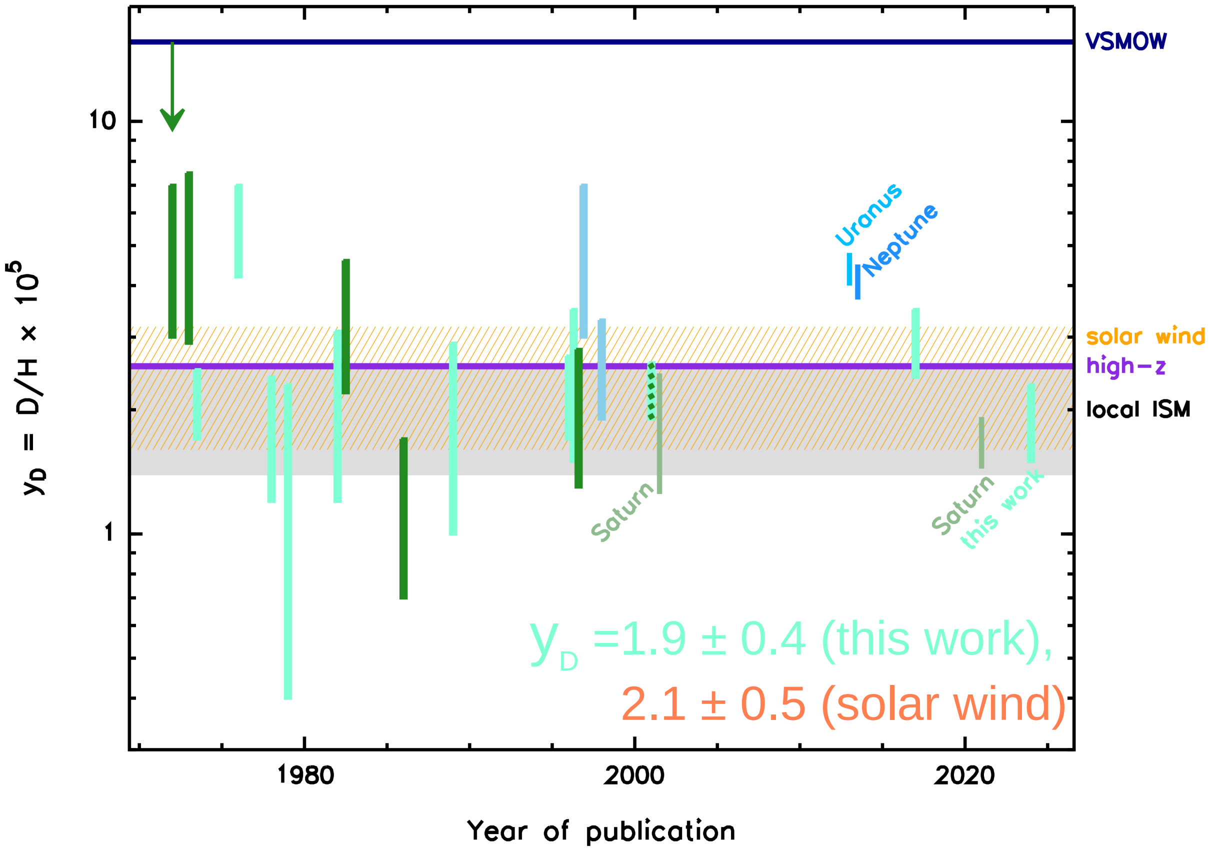

- Solar-wind and HD-derived (λ112 μm) protosolar D/H fractions agree.
- No significant difference between Jupiter and Saturn.

Jupiter D/H fractions derived from CH_3D/CH_4 and $HD/H_2 \approx D/H$.

References:

Solar wind: Gautier & Morel (1997), Geiss & Gloeckler (1998).

High-z: Riemer-Sørensen+ (2017), Cooke+ (2018), Fields+ (2020).

ISM: Linsky+ (1998, 2006), Tsujimoto (2011), Friedman (2023).

Jupiter: Reeves & Bottinga (1972), Encrenaz/Combes+ (1978-1996), Lellouch+ (2001), Galileo mission: Niemann+ 1996, Mahaffy+ 1998.

Synopsis of cosmic deuterium fractions

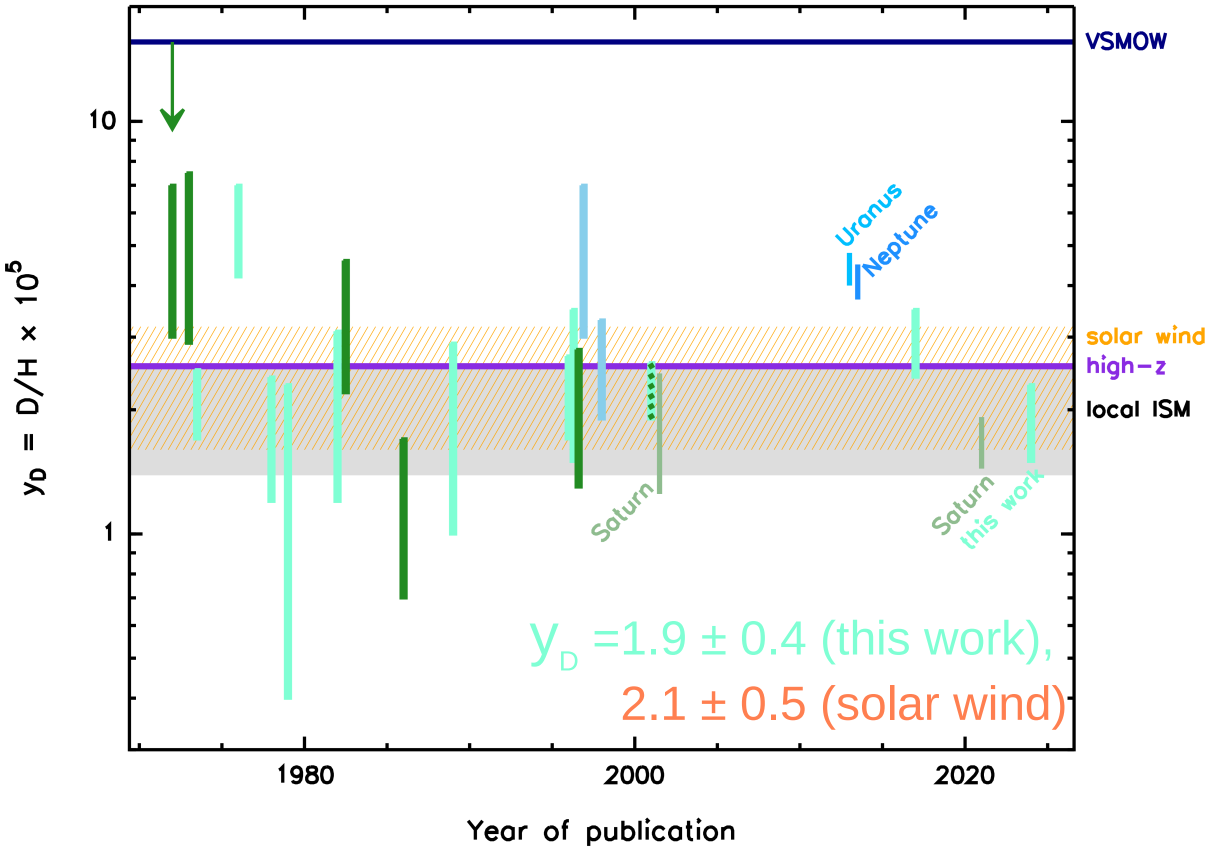

- Solar-wind and HD-derived (λ112 μm) protosolar D/H fractions agree.
- No significant difference between Jupiter and Saturn.

CH_3 + HD ↔ CH_3D+ H, fractionation 1.3

H_2 + D ↔ HD + H, fractionation 1.03

References:

Solar wind: Gautier & Morel (1997), Geiss & Gloeckler (1998).

High-z: Riemer-Sørensen+ (2017), Cooke+ (2018), Fields+ (2020).

ISM: Linsky+ (1998, 2006), Tsujimoto (2011), Friedman (2023).

Jupiter: Reeves & Bottinga (1972), Encrenaz/Combes+ (1978-1996), Lellouch+ (2001), Galileo mission: Niemann+ 1996, Mahaffy+ 1998.

III. Isotopic exchange reactions in Earth's upper atmosphere

Wiesemeyer+ 2023, Phys.Rev.Res.

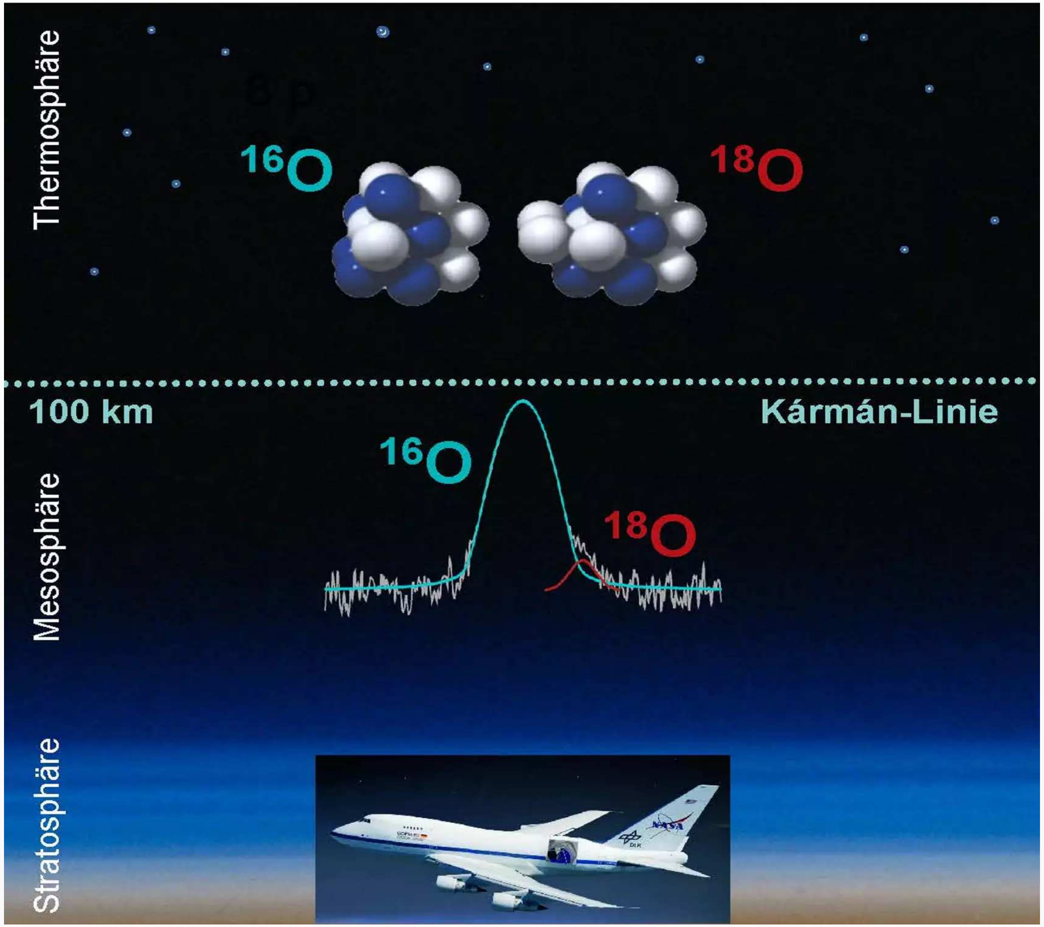

© Wiesemeyer et al./ NASA/ DSI (Stéphane Guisard & NIESYTO design)/ Simmon (NASA GSFC)

Heavy oxygen fraction in Earth's upper atmosphere, non-LTE via isotopic exchange:

$$^{18}O + {}^{32}O_2 \leftrightarrow {}^{16}O^{18}O + {}^{16}O \quad (1)$$

$$^{16}O + {}^{36}O_2 \leftrightarrow {}^{16}O^{18}O + {}^{18}O \quad (2)$$

$$^{18}O(^3P_J) + X' \leftrightarrow {}^{18}O(^3P_J') + X \quad (3),\ X=N_2,O_2,O$$

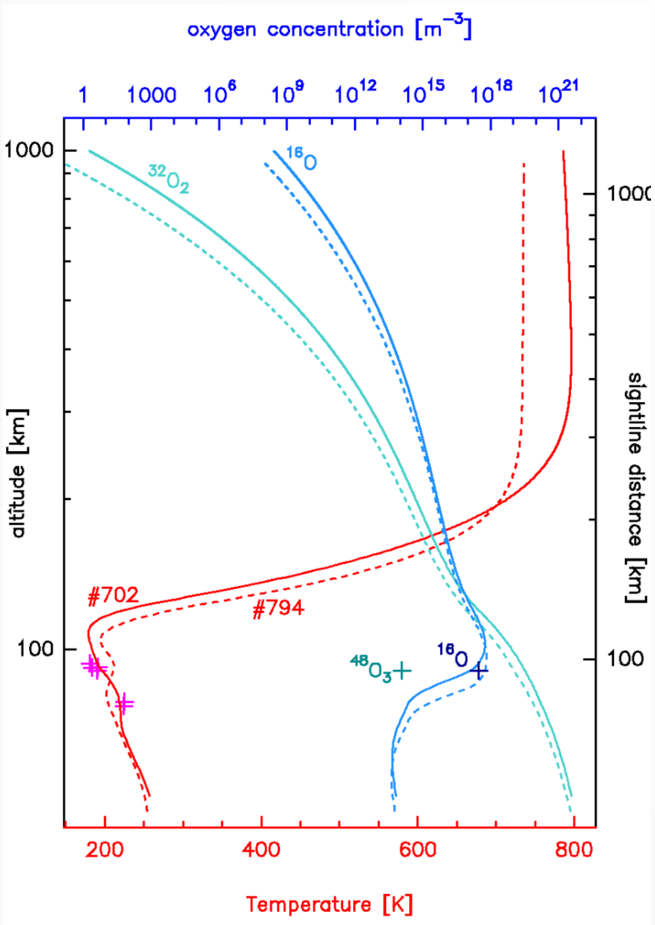

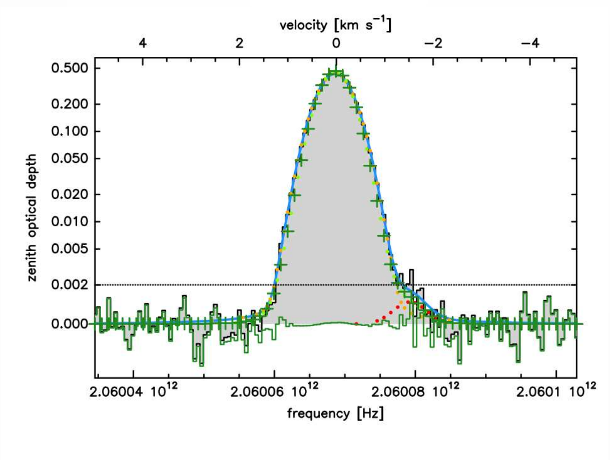

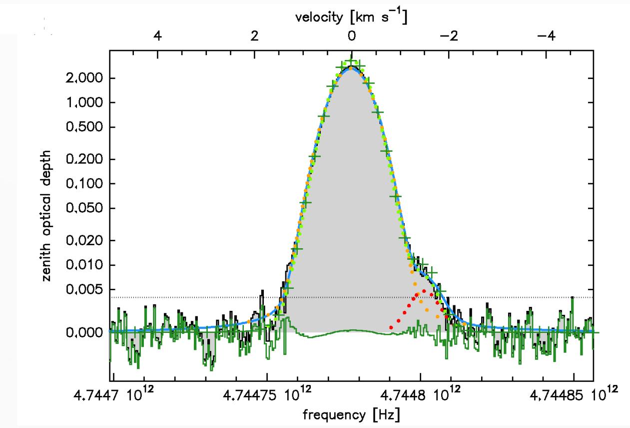

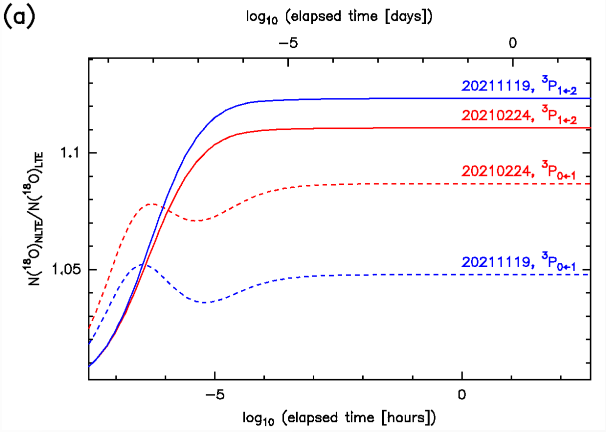

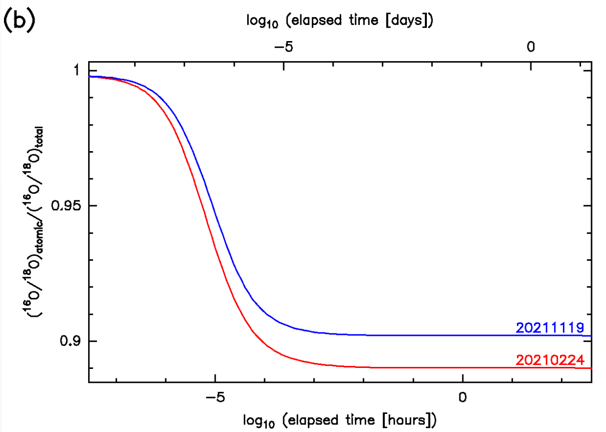

Heavy oxygen fraction in Earth's upper atmosphere, non-LTE via isotopic exchange:

$$^{18}O + {}^{32}O_2 \leftrightarrow {}^{16}O^{18}O + {}^{16}O \qquad (1)$$

$$^{16}O + {}^{36}O_2 \leftrightarrow {}^{16}O^{18}O + {}^{18}O \qquad (2)$$

500x slower

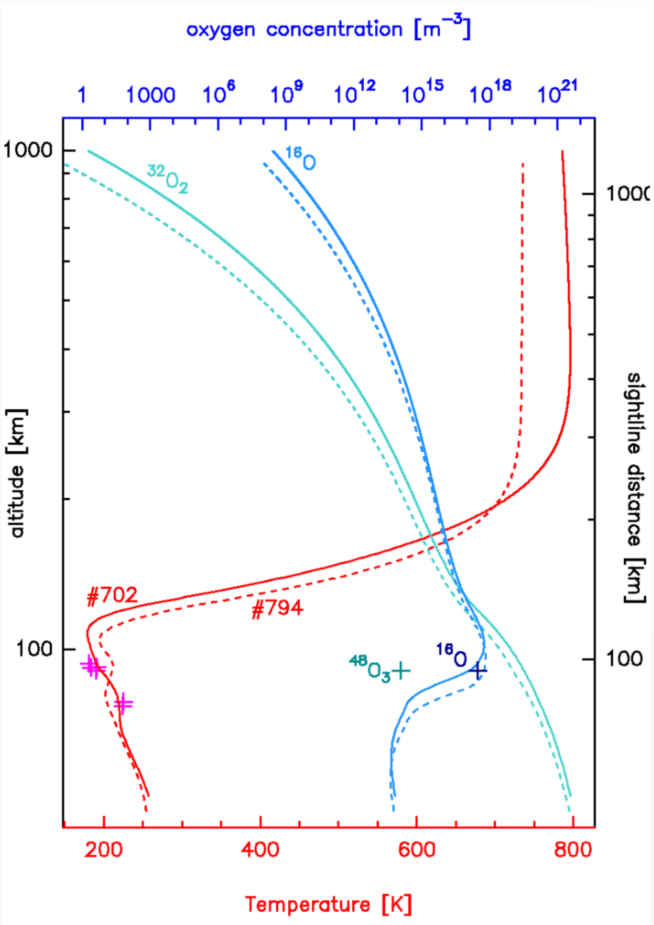

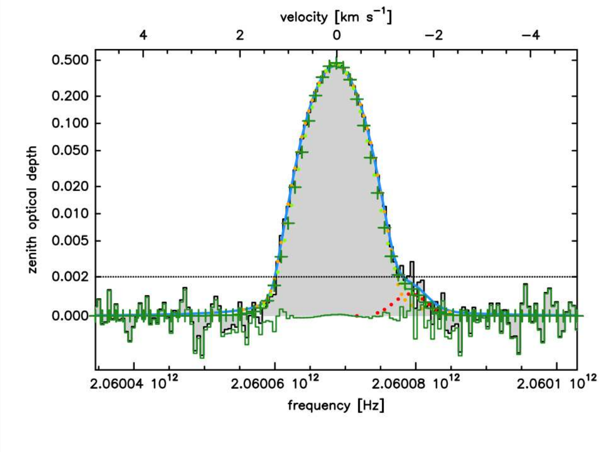

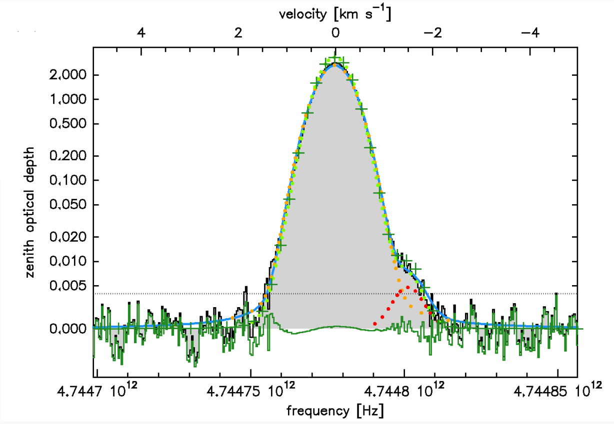

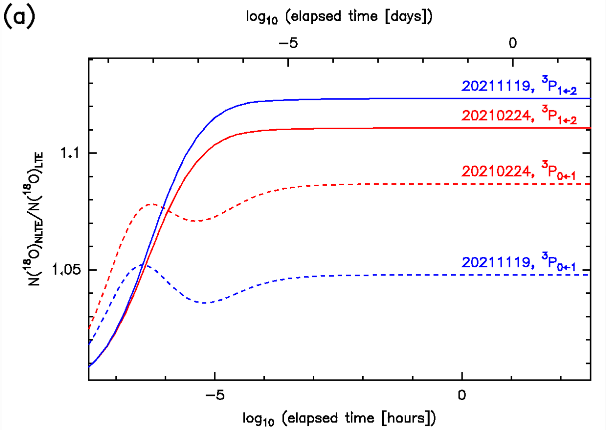

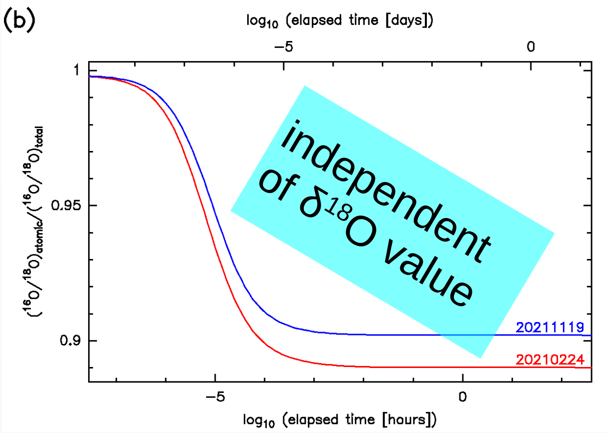

Heavy oxygen fraction in Earth's upper atmosphere, non-LTE via isotopic exchange:

$^{18}O + {}^{32}O_2 \leftrightarrow {}^{16}O^{18}O + {}^{16}O$ (1)

$^{16}O + {}^{36}O_2 \leftrightarrow {}^{16}O^{18}O + {}^{18}O$ (2)

$^{18}O(^3P_J) + X' \leftrightarrow {}^{18}O(^3P_J') + X$ (3), $X=N_2,O_2,O$

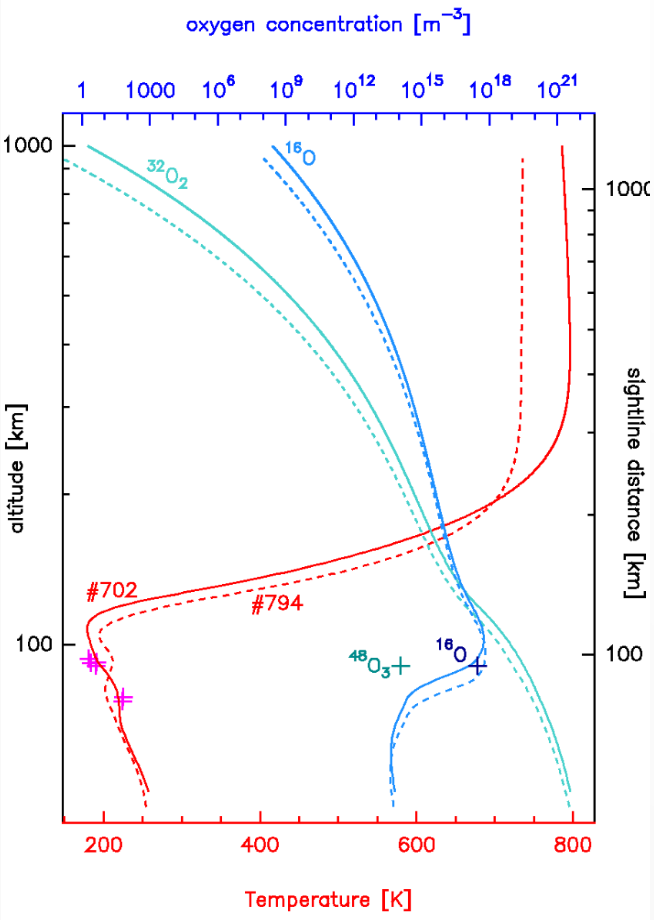

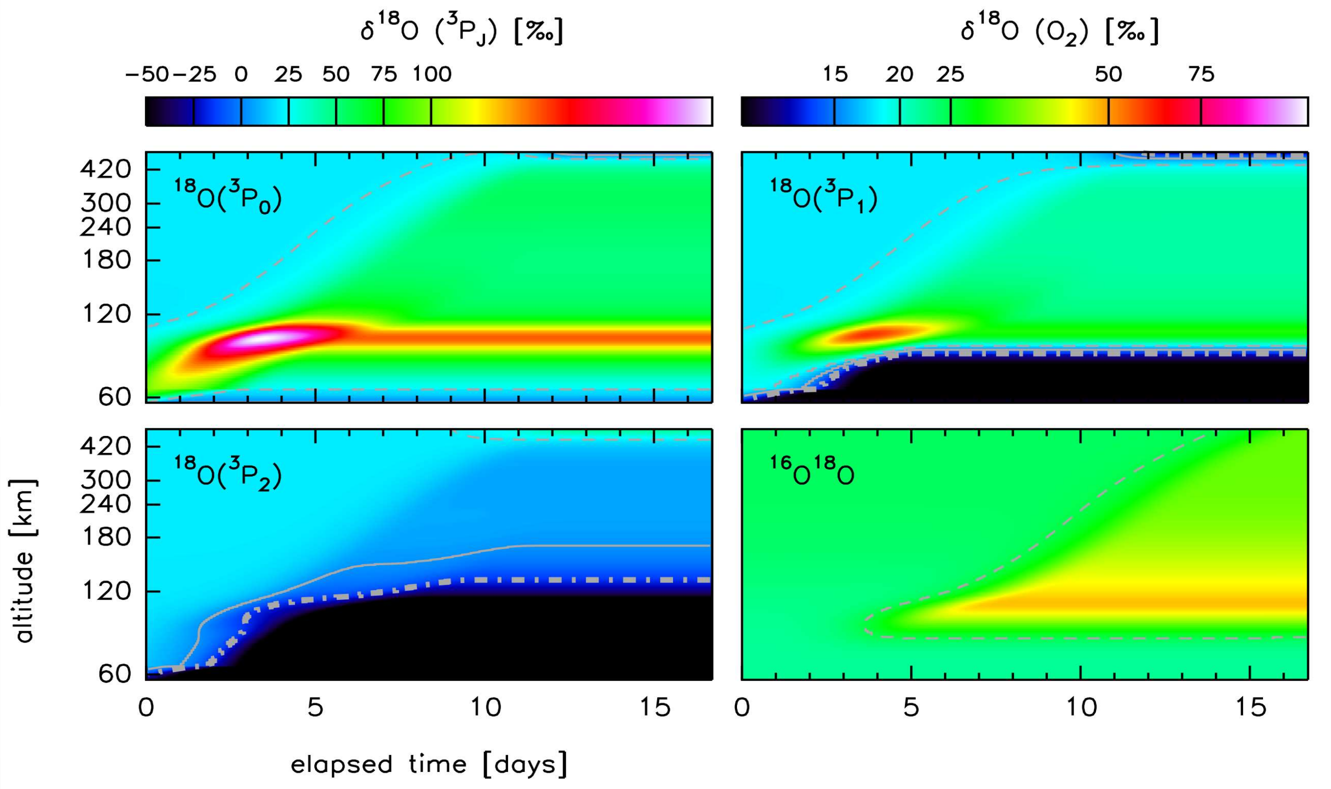

The heavy oxygen fraction $^{18}O/^{16}O$ – a signpost of oxygenic metabolism?

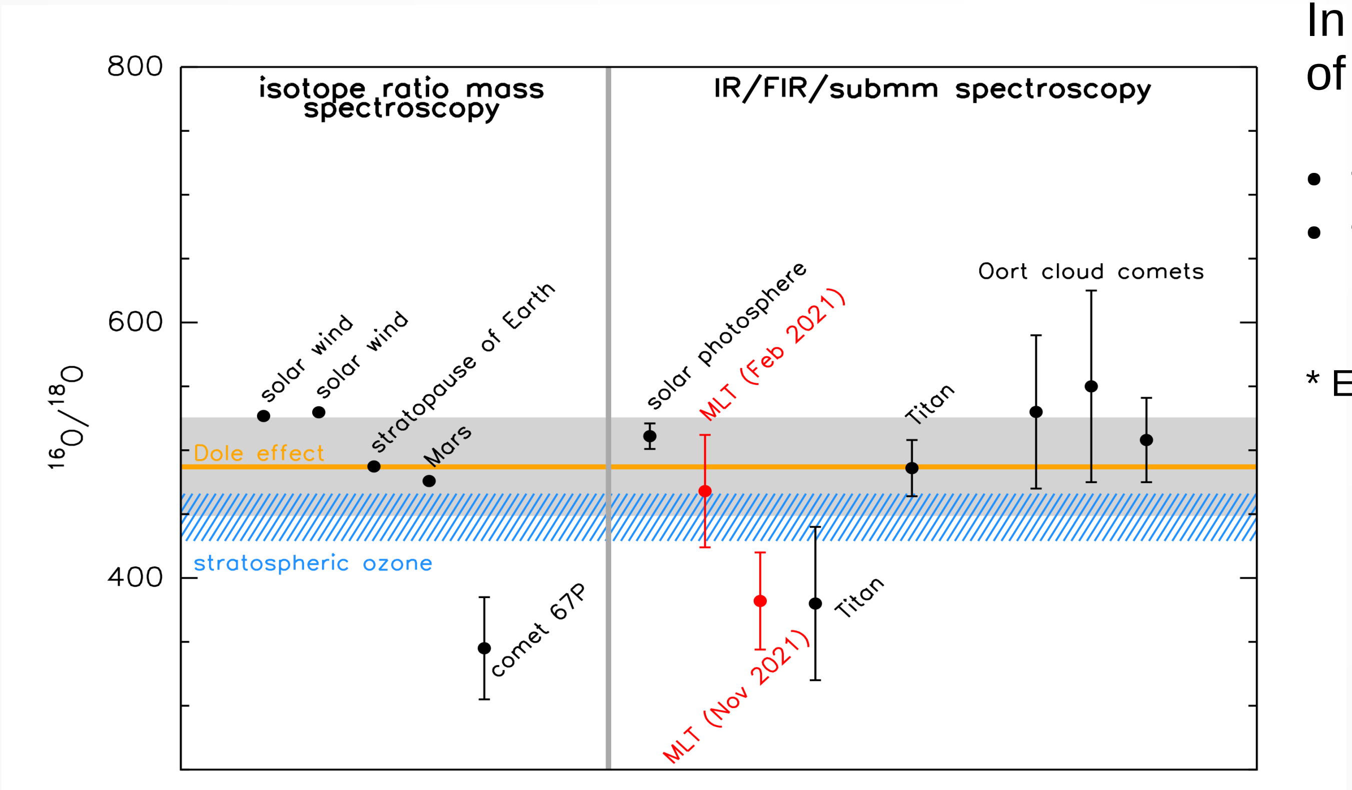

Wiesemeyer et al. (2023), PhysRevRes **5**, 013072

In the mesosphere & thermosphere of Earth, the ^{18}O enrichment

- falls below solar wind value,
- formally agrees with the Dole effect*.

* Equilibrium of respiration & photosynthesis.

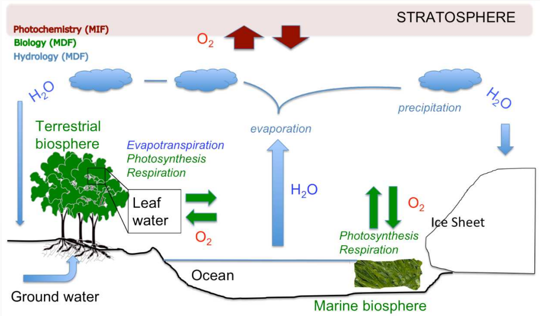

PhD C. Reuteneuer (2016, U.Copenhagen)

Tracer for ocean loss on Venus (cf. ^{16}OI detection, Hübers et al. 2023).

Summary

- Modeling of astrophysical environments requires accurate rates for the chemical pathways to separate reactive and isotope/charge/isomer exchanging collisions from inelastic ones, for applications as varied as

  - HeH^+ as potentially important coolant in the young universe,
  - the protosolar D/H fraction through IR spectroscopy of the gas giants (benefiting from full mapping),
  - thermal disequilibrium in the mesosphere and thermosphere of Earth,
  - isotopically heavy species for tracing ocean loss (Venus, tbd) or biogenic signatures (Earth).

- Analysis requires high-resolution IR spectroscopy and laboratory experiments (state-resolved rate coefficients for the full Maxwell distribution, line-shape parameters).
  See also OH/H_2O branching ratio: observations vs. laboratory measurements (Wiesemeyer+ 2016).

- The same holds in interstellar and star-forming environments, e.g.,

  - spin-isomer exchange in H_2D^+ and H_2 (Brünken+ 2014, L183),
  - fast isotopic exchange between OD & OH in envelopes around high-mass cores (Csengeri+ 2022),
  - the Galactic $^{12}C/^{13}C$ gradient deduced from the isotopologue ratio of CH (Jacob+ 2020).

Synergies

Fundamental spectroscopic parameters and cross sections

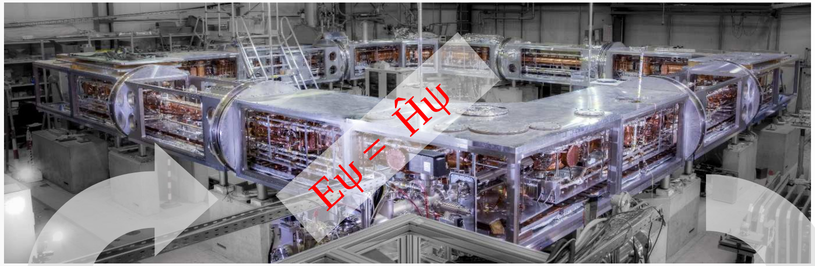

Instrumentation

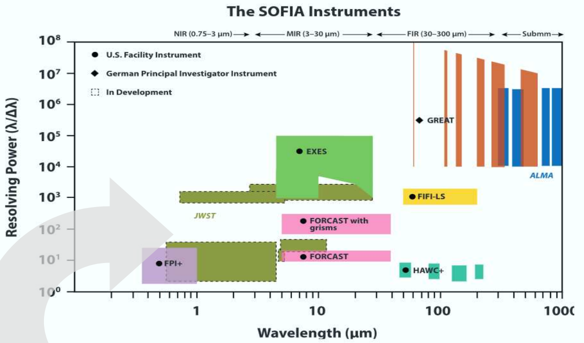

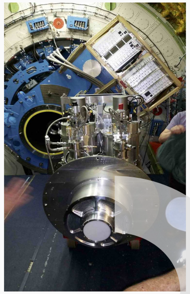

Forward modeling & radiative transfer

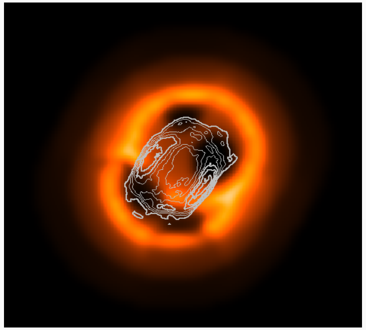

Observing, calibration & data reduction

Thank you!

Fundamental spectroscopic parameters and cross sections

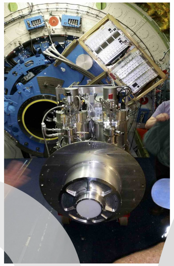

Instrumentation

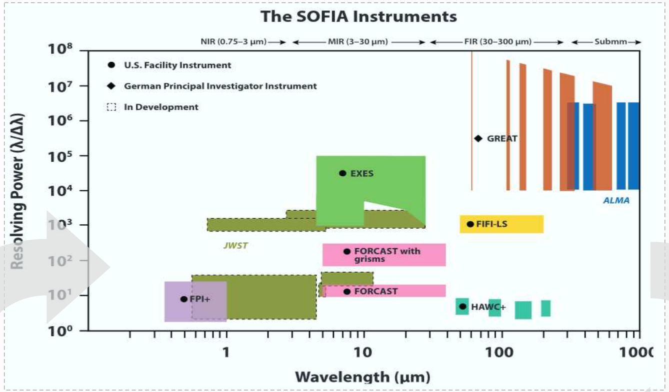

Forward modeling & radiative transfer

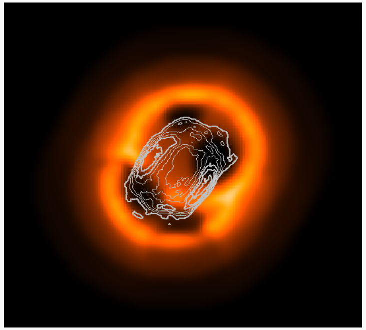

Observing, calibration & data reduction